Psychophysiology

WILEY | SPR Society for Psychophysiological Research

ORIGINAL ARTICLE

Dissociable Effects of Attention and Prediction on Visual Processing: Evidence From Overlap-Corrected Visual ERPs

Maximilien Van Migem[1] | Daniele Marinazzo[2] | Gilles Pourtois[1]

[1]Department of Experimental Clinical and Health Psychology, Ghent University, Ghent, Belgium | [2]Department of Data-Analysis, Ghent University, Ghent, Belgium

Correspondence: Maximilien Van Migem (maximilien.vanmigem@ugent.be)

Received: 15 July 2025 | **Revised:** 15 November 2025 | **Accepted:** 14 December 2025

Keywords: attention | C1 | ERP | linear deconvolution | overlap correction | P1 | P3 | prediction | visual perception

ABSTRACT

Visual processing is influenced by spatial attention and prediction. Yet, in humans, it is still unclear if early sensory processing in the primary visual cortex (V1) is influenced by these top-down factors. To answer this question, various EEG studies have looked at the retinotopic C1 event-related potential (ERP), which arises from V1. Despite the fact that research on this question has been ongoing for more than two decades, discrepant findings have been reported. One reason for this heterogeneity could be due to the majority of studies focusing mostly on attention, without considering the possible role of prediction. Another reason could stem from the C1's specific sensitivities to stimulus features and individual differences. To address these issues, we developed a new paradigm that maximally utilizes the visual and spatial properties of the C1 and allows for the factorial manipulation of spatial attention and prediction. We also used gaze-contingent eye-tracking to confirm the use of peripheral vision to process the stimuli. Additionally, to account for the individual differences in the C1 response the experiment was tailored to each participant using an independent localizer. The ERP results showed a significantly smaller C1 amplitude in the upper visual field when attention was directed toward the peripheral stimulus as opposed to when it was directed away toward the center of the screen. After applying linear deconvolution to correct for temporal overlap between sequential ERP responses, this effect disappeared. We found that attention influenced the P1, while prediction mostly affected the P3. These novel results suggest that early sensory processing in V1 is not directly influenced by either attention or prediction; their effects are dissociable and mostly concern the P1 and P3 ERP components.

1 | Introduction

Visual processing is determined not only by sensory input but also by active goals and prior knowledge (Clark and Hillyard 1996; De Lange et al. 2018; Kok et al. 2014; Luck et al. 2000; Muckli and Petro 2013; Rao and Ballard 1999). As information travels through the visual cortex, it is modulated by top-down processes such as attention and prediction, leading to efficient inferences about the visual environment. Over the last decades, various functional magnetic resonance imaging (fMRI; Aitken et al. 2020; Alink et al. 2010; Kok et al. 2014; Kok, Rahnev, et al. 2012; Richter and De Lange 2019) and animal studies (Debes and Dragoi 2023; Gilbert and Li 2013; Kapadia et al. 1995) have established that this modulation already occurs at least at the level of the primary visual cortex (V1) if not at an even lower level (Lamme and Roelfsema 2000). According to prominent predictive coding theories, sensory input is integrated through the processing of prediction errors (PEs) that are generated along with the transmission of information through various levels of the cortical hierarchy (i.e., feedforward sweep); each level then produces an updating response to that information (i.e., feedback sweep) depending on the size of the PE to thereby adapt the system for future inference (Clark 2013; Friston 2009; Rao and Ballard 1999). However, even though some studies have been able to indirectly differentiate feedforward and feedback

activity by investigating connectivity between cortical layers of V1 (Aitken et al. 2020; Thomas et al. 2024), a direct temporal distinction between these two processes has remained difficult, mainly due to fMRI's sluggish temporal resolution.

To investigate whether V1 is modulated during feedforward processing, various EEG studies have examined the C1 event-related potential (ERP) component. This deflection is the earliest observable electrophysiological response to visual stimuli (≈60–90 ms post stimulus onset) and is sensitive to low-level visual properties that depend on V1, including spatial frequency and luminance contrast (Foxe et al. 2008; Gebodh et al. 2017; Kenemans et al. 2000; Pitts et al. 2010; Proverbio et al. 2010; Rauss et al. 2011). Additionally, the C1 shows a distinctive electrophysiological property that corresponds to V1's anatomy, namely a polarity reversal depending on the position of the stimulus along the vertical axis/meridian. More specifically, the C1 is positive for stimuli shown in the lower visual field (LVF), but negative for the exact same stimuli shown in the upper visual field (UVF), corresponding to the activation of pyramidal neurons above and below the calcarine fissure with opposite orientations, respectively (Clark and Hillyard 1996; Di Russo et al. 2002; Jeffreys and Axford 1972; Kelly, Vanegas, et al. 2013). Accordingly, the C1 ERP component is generally considered an early visual activity arising from V1 following stimulus onset (Foxe and Simpson 2002). While some authors have critiqued this notion by pointing out that polarity reversals can also occur for later components (Ales et al. 2010, 2013), subsequent work has reinforced that the specific, early, and retinotopically precise pattern of the C1 is unique to V1, as is demonstrated in studies leveraging comprehensive visual field mapping (Kelly, Schroeder, and Lalor 2013; Kelly, Vanegas, et al. 2013; Mohr et al. 2024).

After more than two decades of psychophysiology research, the modulation of the C1 amplitude by top-down factors is still a point of contention (Qin et al. 2023). Early studies looking at spatial attentional effects on visual ERPs found that while the P1 (80–120 ms) or N1 (140–200 ms) component, both arising from the extrastriate visual cortex, were modulated by this top-down factor, the preceding C1 was not (Clark and Hillyard 1996; Hillyard et al. 1998; Luck et al. 2000; Mangun et al. 2001). Moreover, studies combining fMRI with EEG have shown that while spatial attention modulated V1, it did not affect the C1 as opposed to the subsequent P1 and N1 components (Martínez et al. 1999, 2001; Noesselt et al. 2002), which is in agreement with a feedback or re-entrant effect from the extrastriate cortex onto the striate cortex. Nonetheless, following these early null findings for the C1, other more recent ERP studies have documented modulations of the C1 by spatial attention or attentional load, especially when taking into account C1-specific properties and minimizing inter-individual differences in V1 anatomy (Dassanayake et al. 2016; Fu et al. 2009; Kelly et al. 2008; Mohr et al. 2020; Wolf et al. 2022; see Slotnick 2018 for a review). For instance, Kelly et al. (2008) were among the first to provide evidence of attentional modulation of the C1. They did so by taking into account the relationship between C1 response and stimulus' spatial positioning resulting from possible neuroanatomical differences. To do this, they used a functional localization procedure to adjust stimulus presentation positions to better correspond to each participant's optimal mapping and found a greater C1 magnitude in the presence of attention. Yet, recent attempts have failed to replicate these results, even when taking individual neuroanatomy into account (Alilović et al. 2019; Baumgartner et al. 2018). In fact, some researchers have argued that null results for the C1 seemingly outnumber positive findings (e.g., Baumgartner et al. 2018). However, in a recent meta-analysis including all C1 studies available in the existing literature and considering different types of attention manipulations, Qin et al. (2022) found moderate evidence (Cohen's $d_z = 0.33$) for a significant modulation of this ERP component by attention, expressed by a larger amplitude for attended compared to unattended stimuli or locations.

One reason that could be contributing to the difficulty of finding systematic top-down modulations on the C1, in addition to neuroanatomical and stimulus specific parameters, is that the vast majority of studies manipulating spatial attention have done so (either endogenously or exogenously) by cueing a specific location in the visual field (either left/right or upper/lower), in keeping with the logic of the Posner task (see Qin et al. 2022; Slotnick 2018). However, a potential problem with this standard approach is that it remains difficult to disentangle the effects of spatial attention from prediction (Doricchi et al. 2022; Summerfield and Egner 2009). This is a limitation because these two processes can yield opposing effects in V1: whereas attention is known to boost, via dedicated gain control mechanisms, neural activity in V1 (Di Russo et al. 2002; Martínez et al. 1999; Noesselt et al. 2002), prediction has been shown to attenuate it in this area (Alink et al. 2010; Egner et al. 2010). In fact, some fMRI studies investigating both factors concurrently have shown that they can yield complex interaction effects on neural activation in the visual cortex, including in V1 (Kok, Jehee, and de Lange ; Kok, Rahnev, et al. 2012; Richter and De Lange 2019). For instance, Kok, Jehee, and de Lange (2012) elegantly manipulated spatial attention by having participants only respond to stimuli appearing in a cued part of the visual field (either left or right) while ignoring stimuli appearing in the other part of the visual field. Prediction, on the other hand, was manipulated orthogonally by altering the likelihood of stimuli appearing in one visual field over the other. They found that for the attended part of the visual field, predicted stimuli had more contralateral activation in V1 and the extrastriate cortex (V2 and V3) compared to unpredicted stimuli. For the unattended part of the visual field, on the other hand, this effect was inversed, namely a larger activation was found for unpredicted compared to predicted stimuli. Activation in the ipsilateral visual cortex (i.e., corresponding to the visual field where stimuli were absent) had the exact opposite pattern.

Despite this, very few EEG studies have examined the possible interaction effect of attention with prediction on early visual processing and more specifically on the C1 component (Alilović et al. 2019; Herde et al. 2018). A notable exception is the study performed by Alilović et al. (2019), who employed many of the same experimental manipulations used by Kelly et al. (2008), including an individualized stimulus presentation and a Posner-like attentional manipulation that consisted of cueing the task-relevant visual field, with the addition of a prediction manipulation (stimulus likelihood) similar to Kok, Jehee, and de Lange (2012), but they reported no effects of either attention or prediction on the C1. However, because both attention and prediction manipulations were aimed at influencing processing of one visual field over the other in their experimental design,

effects on the C1 component would have to depend on lateralized processing. Whereas the use of fMRI allowed Kok, Jehee, and de Lange (2012) to distinguish opposing activation profiles, emerging from attention/prediction interactions, between contralateral and ipsilateral parts of the visual cortex, this complex distinction could be more difficult to observe when looking at the C1 component. For instance, opposing modulations of attention and prediction on contra- and ipsilateral hemispheres could confound the observed effects on centrally measured C1 activity. In fact, research using Posner-like attention manipulations has often found differing effects of attention between ipsi- and contralateral electrodes, particularly on the later P1 and N1 components, which are measured along more lateral occipital regions (Di Russo et al. 2002; Hillyard et al. 1998; Mangun et al. 2001; Marzecová et al. 2017; Noesselt et al. 2002). This is also the case for Alilović et al. (2019) who found a significant P1 attention modulation as well as a marginal effect of prediction, but in both cases only for electrodes contralateral to stimulus presentation and not ipsilateral ones.

In the present study, we aimed to address these limitations when investigating the dynamics of top-down influences on early visual processing in V1. We did so by orthogonally manipulating spatial attention and prediction and quantifying their influence on the C1 component (as well as subsequent visual ERPs). More specifically, we manipulated spatial attention without contrasting the left and right visual fields but instead by directing attention to either the center of the visual field or to the periphery (where the C1-eliciting stimulus was shown). Independently of attention, we also manipulated prediction by altering the likelihood of the stimulus. This prediction concerned the location of the stimulus, as could be inferred based on apparent motion (Ekroll et al. 2008; Kolers 1963). On each trial, four successive visual stimuli were shown in close temporal proximity in the four visual quadrants to produce a specific directional rotation (i.e., the stimulus rotated either clockwise or anticlockwise) that was maintained/reinforced at the block level. Hence, the participants could predict this rotation (i.e., where the next stimulus was shown in the visual field) and this is the very property that we altered, irrespective of attention. Unexpectedly, on some trials during the block, an opposite rotation unfolded (e.g., instead of clockwise, the stimulus rotated anticlockwise). We employed this because apparent motion has been shown to affect predictive processing in V1 in previous fMRI studies (Alink et al. 2010; Muckli and Petro 2013). In addition, we also took into account the variability of C1 responses due to individual neuroanatomy by adjusting stimulus presentation to correspond to each participant's optimal C1 signature. We assessed if attention, prediction or their interaction effect could influence the C1, but also the subsequent ERP components (P1, N1 and P3).

2 | Methods

2.1 | Participants

In their meta-analysis, Qin et al. (2022) reported a mean Cohen's d of 0.33 for attentional effects on the C1. Using it as a prior, we made a power estimation using G*Power (Faul et al. 2007), which indicated that 18 participants were needed to find a similar effect size with a within-subject repeated measures ANOVA and a power of 0.9. We therefore aimed to collect data from at least 18 participants resulting in the recruitment of 26 participants in total, after accounting for participant drop-out. All participants were recruited via Sona Systems, which is an online recruiting tool used by Ghent University. We excluded one participant from the analyses because of EEG recording issues. Two others were excluded because we could not record eye movements. Lastly, the experimental session was cut short for two other participants. This led to the partial loss of data, more specifically when these participants were attending the periphery (see below). The remaining data, however, was still included in the final analyses, which consisted of data from 23 participants (15 female, mean age: 24.3, SD: 7.0, 19 righthanded), all of whom had normal or corrected-to-normal vision. The study was approved by the local Ethics Committee of the Faculty of Psychology and Educational Sciences at Ghent University; all participants gave written informed consent and were rewarded 30 Euros for their participation.

2.2 | Apparatus

The experiment took place in a dimly lit, electrically shielded room. Participants were seated in front of a 19′ inch CRT monitor with a refresh rate of 75 Hz at a 1600×1200 resolution. To restrain movements and to set the distance from the screen fixed at 63 cm, a chin rest was used. Stimuli were generated and presented using Python 3.8 and Psychopy v2022.2.4 (Peirce et al. 2019) on a Dell Optiplex 7090 mini-tower (CPU i5-10,600, 16 GB RAM). Eye movements were continuously recorded at 1000 Hz using an SR-research Eyelink 1000 plus system. Electrophysiological data were collected with a 64-channel BioSemi ActiveTwo system at a sampling rate of 512 Hz and positioned according to the extended international 10–20 system. CMS-DRL electrodes were used as online reference. Lastly, four electrooculograms were placed: on the left and right canthi for the detection of horizontal eye movements, and above and below the left eye for the detection of blinks.

2.3 | Stimuli and Design

In each trial, a stimulus was peripherally presented four times, once in each quadrant of the screen (i.e., top left, top right, bottom right, and bottom left). The presentation pattern was designed to induce an apparent rotational motion (Alink et al. 2010; Ekroll et al. 2008; Kolers 1963) with the stimulus appearing sequentially in either a clockwise or anticlockwise direction (see Figure 1A) around a central fixation cross (width: 0.75° VA). This rotation was used to manipulate prediction by having one direction (regular condition: 75% of trials) be more frequent than the other one (odd condition: 25% of trials) throughout the experiment. For half of the participants, the regular rotation direction was clockwise and the odd direction was anticlockwise, while the reverse mapping was true for the other half. It is important to note that at the trial level, the first moment where a violation of prediction could be detected was the presentation of the second stimulus (of the rotation), and this stimulus was therefore expected to elicit the strongest PE. To be able to compare specifically this second stimulus between regular and odd trials, the experiment had two diametric starting positions (i.e., top left/

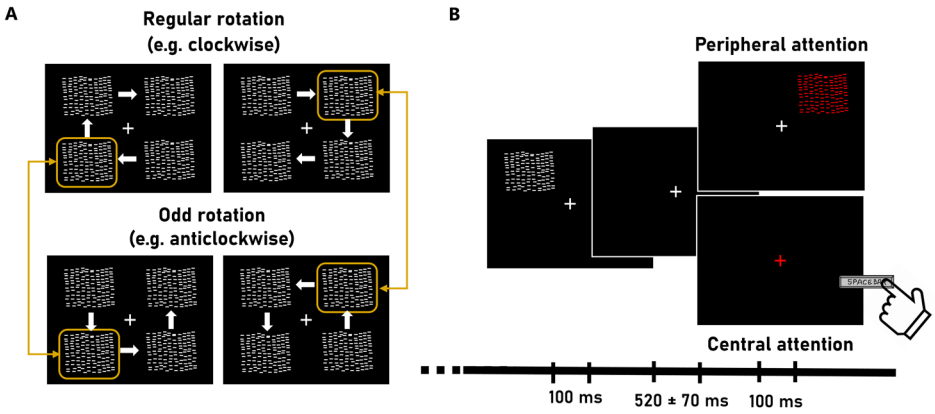

FIGURE 1 | Experiment design. (A) On every trial, a stimulus designed to elicit a strong C1 response appeared sequentially in each quadrant of the screen. The order of the sequence was designed to induce rotational motion, either clockwise or anticlockwise. One of these rotation directions was more frequent (75%) than the other one (25%). Two different starting positions of the stimulus in a trial depended on the individual C1 response and alternated every 7–8 blocks. The location of the second stimulus in each trial depended on the rotation direction and the starting position. The different starting positions allowed for the comparison between predicted and unpredicted rotation when the second stimulus was in the same spatial location (indicated by the orange outline). On the figure, the arrows are used to indicate the direction of the rotation, but they were not used during the experiment (B) A target appeared in 3% of trials. In one part of the experiment (peripheral attention), this target was the peripheral stimulus in red instead of white and in the other part (central attention), the target was the fixation cross turning red for the duration of one stimulus presentation (100 ms).

bottom right or top right/bottom left) so that in trials with a different starting position, the second stimulus would appear in the same spatial position in clockwise and anticlockwise rotations. The starting positions were determined individually for every participant by a localizer prior to the start of the main experiment (see procedure).

Attention was manipulated by having participants either attend to this peripheral stimulus or the fixation cross. We did this by including a target detection task in which participants had to respond as quickly as possible by pressing the spacebar when the peripheral stimulus turned red in one condition (peripheral attention) or when the fixation cross turned red in the other condition (central attention). More precisely, in the peripheral attention condition, the stimulus would appear red instead of white, only once within a trial, and with the same probability for any of the four quadrants. In the central attention condition, the fixation cross, which stayed on screen, would turn red for the duration of one of the stimulus presentations in a trial. Importantly, these targets were very infrequent, only occurring in 3% (26 trials) of the total trials (840 trials; see Figure 1B). These conditions did not overlap, meaning that in the peripheral attention condition, only the stimulus could turn red whereas in the central attention condition, only the fixation cross could turn red. Half of the participants were assigned to the peripheral condition in the first part of the experiment and the central condition in the second part, with this order being reversed for the other half of the participants.

The peripheral stimulus was specifically designed to elicit a robust C1 response and consisted of an array (width: 6° VA) with a high spatial frequency of 12 by 10 white horizontal lines (length: 0.76° VA, width: 0.04° VA) on a black background (Qin et al. 2023). This texture created a strong contrast and was accompanied by edge effects because each line had a slight offset (±0.08° VA). The stimulus used throughout the experiment was always the same (except for turning red during target trials) and was presented at a fixed distance of 8.36° VA from the fixation cross to the center of the array.

2.4 | Procedure

After receiving a short briefing, filing in the consent form, and undergoing EEG preparation, participants were seated in the testing chamber where they had to fill in their demographic information and select their preferred instruction language (either Dutch or English). In the chamber, they received further instructions about the eye-tracker calibration and the need to maintain fixation throughout. The experimental session consisted of two parts: a localizer and the main experiment. The localizer entailed the presentation of the same stimulus with the same duration and inter-stimulus interval (ISI) (see below) as the main experiment but without the main experimental manipulations. The stimulus was thus presented in a completely random pattern (i.e., without recurrent rotation and with some repetitions possible), without the division of four stimulus presentations per trial and under passive viewing conditions (i.e., no target detection task). The purpose of the localizer was to identify the quadrant for each participant that elicited the strongest C1 response so that the main experiment could be adjusted to correspond to this optimal quadrant (i.e., to have the second stimulus that belonged to the rotation sequence in the main experiment appear at this specific location). As mentioned above, there were two different starting positions and as a result, there were two positions where the critical prediction manipulation occurred (i.e., the presentation of the second stimulus of the trial; see Figure 1A). The starting positions (i.e., top left/bottom right or top right/bottom left) were selected individually for each participant so that one of these critical positions coincided with the participants' optimal C1 quadrant. Additionally, the localizer data were used for C1 peak selections in the main analyses

and for electrode selection in the individualized C1 analysis (Kelly et al. 2008). The data of the localizer were pre-processed and analyzed online prior to the start of the main experiment (see below).

The main experiment was divided into 30 blocks, each containing 28 trials. Every trial, the stimulus was presented four times, each time for 100 ms followed by an ISI randomly varying between 450 and 590 ms derived by drawing random integers from a uniform distribution. Trials were separated by an additional 500 ms inter-trial interval (ITI). The duration of the ISI was based on prior deconvolution estimations using simulated data (see section on linear deconvolution). Between every block, participants could take a short break during which they saw a screen displaying their performance thus far (total number of hits and misses). The first 15 blocks consisted of one attention condition (either central or peripheral), and the last 15 blocks consisted of the other attention condition. In between these two sections, a longer break was provided, after which the eye tracker was recalibrated. The first 7 or 8 blocks of each section had one of the two individualized diametric starting positions; the remaining 7 or 8 blocks of the section had the other position. For instance, if in the first 7 blocks each trial started with a stimulus being presented in the bottom left quadrant, then in the next 8 blocks of this session, each trial would start with a stimulus being presented in the top right quadrant.

In a previous EEG study, small and unintentional gaze drifts were shown to influence the C1 amplitude and mask effects of attention (Wolf et al. 2022). To overcome this problem, we implemented a gaze contingent presentation of the first stimulus (of each trial). Prior to each trial, the gaze position of the participant was tracked and needed to fall within a 2.61° by 2.61° VA square around fixation for at least 300 ms (included in the ISI) to initiate stimulus presentation. As long as these conditions were not met (i.e., proper fixation), the trial did not start. If this took longer than 10 s, recalibration was initiated. This same protocol was employed during the localizer before every presented stimulus instead of before every trial.

Because target trials occurred very infrequently, we also ran a behavioral experiment (in a different sample of participants) where this ratio was increased and we could assess the success of the prediction manipulation at the statistical level (see Data S1).

2.5 | EEG (Pre)processing

All pre-processing steps were completed with the MNE-Python toolbox v1.3.1 (Gramfort 2013; Larson et al. 2023). The data were first re-referenced to the joint left and right mastoids. The next steps consisted of a zero-phase notch filter of 50 Hz to remove line noise, a high-pass filter of 0.1 Hz to remove slow-drift and then a low-pass filter of 85.5 Hz to avoid a reduction in temporal precision when down sampling later on. Raw time courses were plotted to visually inspect whether some channels were excessively noisy. Longer spans of data where multiple channels were excessively noisy were also annotated so that these segments could be ignored during the independent component analysis (ICA) and excluded when epoching (see Table 1). Consistently noisy channels were selected and interpolated based on the data from neighboring electrodes (spline). After interpolation, the data were downsampled to 256 Hz. Artifact rejection was done using ICA (*n* components: 0.99 signal variance, method: "fastica") by visually inspecting component topographies for each participant. Components corresponding to blinks and components attributing most variance to a single channel were manually rejected. Lastly, for the standard analyses but not for the overlap corrected analyses (see below), epochs were created from −100 to 450 ms relative to stimulus onset and these were baseline corrected (−100 to 0 ms).

The online processing of the localizer data required a quicker and slightly simplified preprocessing pipeline, which included many of the same steps as the main dataset with the exception of the artifact rejection. Instead of using ICA, blinks were detected with the electrooculogram and spans of data overlapping with this detected blink activity were removed. Additionally, only the Oz POz and Pz channels were visually inspected for excessive noise. After this, stimulus-locked ERPs were plotted for every quadrant. The quadrant showing the largest peak within a 50–100 ms time window across the three aforementioned channels was then assigned as the participants' optimal quadrant. Afterward, the localizer data were processed in the same way as the main dataset.

TABLE 1 | Means and standard deviations of the number of epochs retained after each processing step.

Epoch selection steps	Regular		Odd	
	M	**SD**	***M***	**SD**
Total recorded epochs				
Peripheral	1218.8	124.7	406.3	42.1
Central	1260.0	0.0	420.0	0.0
After artifact rejection				
Peripheral	1217.3	125.5	405.9	42.1
Central	1251.7	35.1	417.5	11.7
Without target trials				
Peripheral	1180.2	122.8	392.8	39.8
Central	1212.0	32.7	405.5	13.1
Second stimulus only				
Peripheral	295.3	30.6	98.3	10.0
Central	303.3	8.2	101.4	3.3
Condition matching				
Peripheral	94.9	9.8	98.3	10.0
Central	97.8	3.0	101.4	3.3

Note: Epochs correspond here to trials, bearing in mind that a trial consisted of four successive visual stimuli. In the main analyses, only the second stimulus in every trial was selected. To achieve comparable signal-to-noise ratios at the ERP level between the odd and regular conditions, we selected regular trials that preceded odd trials (see Condition matching).

2.6 | Data Analysis

Statistical analyses were performed in R (R Core Team 2022) using linear mixed-effects regression (LMER) models from the lme4 package (Bates et al. 2015) and using the LmerTest package (Kuznetsova et al. 2017), which provides *p*-values based on Satterthwaite and Laplace approximations of the degrees of freedom. All categorical dependent variables in this study had two levels and were coded using contrast coding. For all statistical analyses, models were initially fit maximally, meaning that the random structure of the model included a random slope for every independent variable that was also included as a fixed effect as well as a random intercept per participant, in order to avoid the inflation of type-1 errors (Barr et al. 2013). However, some of the maximal models had singular boundaries. This indicates that part of the variance in the random effect structure is close to zero. In order to balance type-1 error inflation with model power (Matuschek et al. 2017), we employed a model selection procedure where random effects were systematically removed (starting with the variables accounting for the least amount of variance) until a simplified model was found that no longer contained a singular boundary. The maximal and the simplified model were then compared on the basis of standard model fit metrics (AIC, BIC and log likelihood) and if these metrics were inconclusive, then we used various other measures (e.g., linearity, homogeneity of variance, collinearity and normality of residuals), provided by the performance package in R (Lüdecke et al. 2021). These latter measures were checked for all models to ensure that there were no clear violations of model assumptions. As mentioned above, we mostly focused on the second presentation of the stimulus for each trial as this stimulus manifested either confirmation or violation of the prediction. To match the trial count between the regular and odd conditions, we subsampled epochs by only selecting regular trials that preceded odd trials (see Table 1).

2.6.1 | Behavior

Although target trials were very infrequent, we did analyze and compare reaction times (RTs) for hits between the central and peripheral attention condition. These RTs were modeled with attention as a fixed effect and with a random intercept for each participant. There were not enough data points to compare effects of prediction on RTs. This analysis was however performed for the control behavioral experiment (see Data S1). We also compared accuracy across conditions by calculating d prime (d′) values from the Signal Detection Theory (SDT; Hautus et al. 2021; Simpson and Fitter 1973) for every condition per participant based on hit-rate and false alarm-rate. Hit-rate was calculated as the number of trials where participants correctly pressed the spacebar within 1000 ms of a target appearing divided by the total number of target trials. False alarm rate was calculated as the number of trials where participants pressed the spacebar when there was no target, divided by the total number of nontarget trials. Because hit-rates for some participants were 100%, we applied a loglinear correction to all individual values to adjust for extreme ones (Hautus 1995). We also calculated the beta parameter, based on the same loglinear corrected hit-rates and false alarm-rate, to assess whether the response bias might differ between conditions. Trials where the target occurred on the first stimulus of each trial were excluded as these did not differ between prediction conditions. These d′ and beta values were then modeled with attention and prediction as fixed effects and with a random intercept for each participant.

2.6.2 | C1

In addition to the influence of experimental factors, top-down effects on the C1 component have also been found to be dependent on the analysis approach, specifically in the way that inter-individual differences are addressed (Kelly et al. 2008; Proverbio et al. 2007). In addition to this, early evoked potentials are particularly vulnerable to distortion resulting from overlap between temporally adjacent ERPs, which has led some researchers to use sophisticated deconvolution methods to correct for overlapping neural activity in the past (Ehinger and Dimigen 2019; Rossi and Pourtois 2012, 2014; Smith and Kutas 2015; Woldorff 1993). However, among the C1 literature, approaches addressing this issue differ significantly from one study to the next, with some opting for shorter variable stimulus onset asynchronies (SOA) using deconvolution methods (e.g., Fu et al. 2010; Hillyard et al. 1998) while others opting for longer SOAs without overlap correction (e.g., Alilović et al. 2019; Kelly et al. 2008; Wolf et al. 2022). To be able to compare the effects of differing approaches to individual variability and to event overlap, we analyzed the C1 in four different ways. We started by comparing a standard ERP analysis with a more individualized analysis. Afterward, we performed these analyses using data that was corrected for overlap through linear deconvolution, using the Unfold toolbox (Ehinger and Alday 2025; Ehinger and Dimigen 2019).

First, in the standard analysis, the C1 amplitude was calculated based on the grand average peak of the occipital parietal electrode (POz) from the localizer data. More specifically, the C1 peak was identified as the maximum absolute amplitude value across four positions between 60 and 90 ms post stimulus onset in the localizer data. The C1 amplitude was scored as the mean amplitude within 20 ms around this peak (89 ms), for each subject per condition in the main dataset. Next, we performed an individualized analysis by selecting the optimal electrode for the C1 response per subject as well as selecting the amplitude window based on the individual C1 amplitude. This meant that the peak C1 amplitude was evaluated separately for each subject by taking the maximum amplitude between 60 and 90 ms post stimulus onset (also the absolute value across four localizer positions). This peak amplitude measure was selected from a set of occipital parietal electrode channels (O1, Oz, O2, PO3, POz, PO4, P1, Pz, P1, CP1, CPz, or CP2) instead of only POz, thereby selecting a peak latency ($M = 0.085$, SD = 0.006 ms) and an optimal electrode for each subject separately. The C1 amplitude in the main dataset was then scored the same way as in the standard analysis (mean amplitude within 20 ms window around the individually localized peak).

In the current design, we examined neural responses to two diametrically opposed spatial positions (i.e., top left/bottom right or top right/bottom left) which were always in opposite visual fields (i.e., UVF or LVF). Consequently, the resulting C1 responses had opposite polarities. We addressed this by including

Visual field (upper vs. lower) as an independent variable in every analysis of C1 amplitude. Thus, for both the standard and the individualized analyses, LMER models were first maximally fit with C1 amplitude as the dependent variable, Attention (peripheral vs. central), prediction (regular vs. odd), Visual field (upper vs. lower), and all two-way and three-way interactions were fitted as fixed effects. Lastly, random slopes were included for all independent variables as well as a random intercept for each participant. Significant interactions between Attention or Prediction and Visual Field were followed up with separate models for UVF and LVF.

As mentioned above, temporally adjacent events can cause overlapping neural responses, leading to the contamination of early visual ERPs, including the C1, by ERPs from preceding events such as other stimuli or motor responses. This contamination gets more pronounced when shorter SOAs are used (as used here in this experiment). Therefore, to control for this, we used the Unfold toolbox (Ehinger and Alday 2025; Ehinger and Dimigen 2019) in Julia (Bezanson et al. 2017), which provides regression event-related potentials (rERP) by fitting linear regression models of neural responses to events on continuous EEG data. Because event onset times are variable, the rERPs of differing event types can then be linearly deconvoluted, resulting in the removal of overlapping activity (Ehinger and Dimigen 2019). We used a finite impulse response (FIR) basis function, which allows for the modeling of any linear overlap shape, with a −100 ms to 1000 ms estimation window. This estimate depends on the assumed length of the underlying EEG activity; a window that is too short might introduce bias by not capturing the entire neural response, while a window that is too long could introduce artifacts due to overfit (see Skukies and Ehinger 2023). This regression resulted in rERPs (consisting of multiple timeseries of regression model coefficients across this −100 ms to 1000 ms time window) for every type of event (e.g., stimulus or motor response) for every condition. We repeated this step for every electrode and every subject and selected only the rERPs corresponding to the second stimulus of each trial. The data were then baseline corrected and analyzed in the same way as described above (i.e., standard and individualized analysis).

2.6.3 | P1, N1, and P3

In addition to the C1 component, we also investigated whether attention and prediction could influence later visual ERPs, focusing on the P1, whose amplitude varies with selective attention (Alilović et al. 2019; Clark and Hillyard 1996; Luck et al. 2000; Wolf et al. 2022), but also the N1 that reflects visual discrimination and is also influenced by spatial attention (Hillyard et al. 1998; Mangun et al. 2001). In addition, we also scored and analyzed the P3, as previous studies have linked it to predictive coding (Knight et al. 1989; Marzecová et al. 2017; Polich 2007). All these components were computed on overlap corrected rERPs (see Data S1 for the analyses of uncorrected ERPs).

As opposed to the central, occipito-parietal C1 component, the P1 and N1 components showed a more lateralised topography. We therefore used two sets of lateral occipital and temporal electrodes (PO3/P07/01 and PO4/P08/02) for the P1 component and two more sets of parietal electrodes for the N1 (PO3/P3 and PO4/P4) and calculated peak latencies per subject. We looked at a positive peak between 100 and 150 ms for the P1 ($M = 132$, SD = 20 ms) and at a negative peak between 150 and 200 ms for the N1 ($M = 178$, SD = 20 ms) for every subject individually. Amplitudes were then computed by taking the average within a 30 ms window around the individual peaks. Both P1 and N1 amplitudes were then modeled using an LMER function with attention and prediction as fixed effects (including interactions) and random slopes, and participant as a random intercept.

As mentioned above, various studies employing Posner-like attention manipulations (left vs. right) have found differences in attentional effects in electrodes that are contralateral to the presented stimulus as opposed to ipsilateral (Alilović et al. 2019; Di Russo et al. 2002; Hillyard et al. 1998; Mangun et al. 2001; Marzecová et al. 2017; Noesselt et al. 2002). We therefore conducted an additional control analysis where we separated the two sets of lateral occipital and parietal electrodes for P1 (PO3/P07/01 and PO4/P08/02) and N1 (PO3/P3 and PO4/P4) and calculated peak latencies separately depending on hemisphere (contralateral and ipsilateral) per subject (P1—contralateral: $M = 122$, SD = 20 ms, ipsilateral: $M = 119$, SD = 19 ms; N1—contralateral: $M = 182$, SD = 20 ms, ipsilateral: $M = 179$, SD = 19 ms). Both P1 and N1 amplitudes were then modeled using a LMER function with attention, prediction and hemisphere as fixed effects (including interactions) and random slopes, and participant as random intercept.

For the P3 component, we selected a subset from a cluster of centro-parietal electrodes (i.e., C1, Cz, C2, CP1, CPz, CP2, P1, Pz, P2, POz) based on the topography and scored it within the 300 to 450 ms window following stimulus onset. The mean amplitude was calculated within this 100 ms window around the peak ($M = 357$, SD = 44 ms) and modeled in an LMER function with attention, prediction, and their interaction as fixed effects, a random slope for each independent variable, and participant as random intercept.

3 | Results

3.1 | Behavior

3.1.1 | RTs

There were no significant differences (beta = 16.23, 95% CI = [−12.31, 44.78], df = 22, $t = 1.114$, $p = 0.277$). Nonetheless, the peripheral targets led to slightly slower RTs ($M = 559.1$, SD = 194.5) than central targets ($M = 526.6$, SD = 157.1).

3.1.2 | SDT

Analysis of d' revealed a significant main effect of prediction (beta = −0.27, 95% CI = [−0.39, −0.16], df = 64, $t = -4.65$, $p < 0.001$), with a larger d' value for targets occurring during trials with a regular direction ($M = 3.82$, SD = 0.65) than for trials with an odd direction ($M = 3.27$, SD = 0.63), but no effects of attention or interactions (all $p > 0.5$). In the control behavioral experiment where target probability was increased, we also

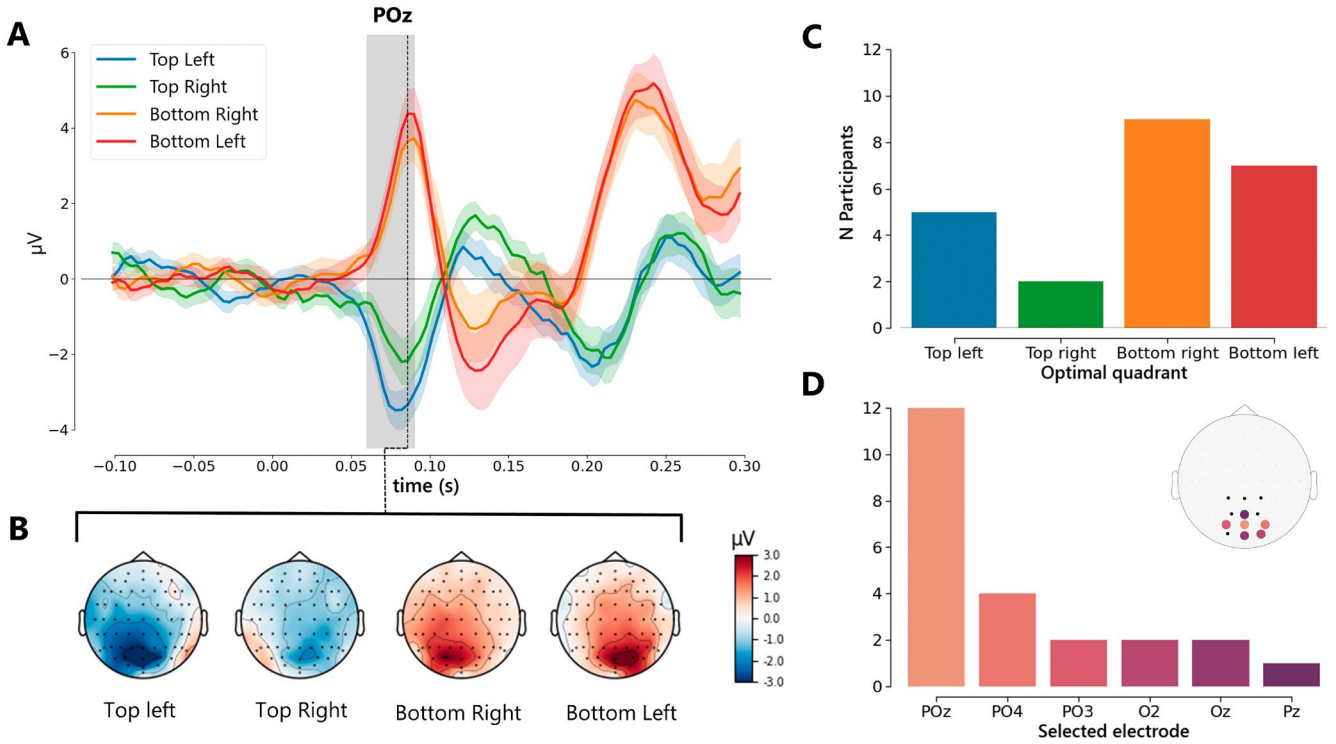

FIGURE 2 | Localizer results. (A) The grand average ERP waveforms at the POz electrode are shown, separately for each position. The gray area shows the range (60–90 ms) wherein peak amplitudes were selected. The dotted line shows the peak latency (89 ms) of the C1 that was used to determine the mean amplitude measurement (standard analysis). Error bands represent the standard error of the mean. (B) The average topographies for each position at the mean peak latency and the corresponding horizontal voltage maps are shown. (C) Bar plot represents distribution of optimal quadrants among participants. (D) Bar plot shows the distribution of optimal electrodes among participants with the corresponding topographical representation.

observed the same effect (see Data S1). The beta values indicating response bias showed a similar pattern, with a significant main effect of prediction (beta = −7.67, 95% CI = [−10,19., −5.15], df = 64, $t = -5.99$, $p < 0.001$), with a larger beta for regular ($M = 33.21$, SD = 18.36) than for odd trials ($M = 17.97$, SD = 5.25), and no significant attention or interaction effects (all $p > 0.3$).

An exploratory follow-up analysis comparing attention conditions separately found this effect on d' to be robust, as a significant difference remained visible in both peripheral (beta = −0.27, 95% CI = [−0.39, −0.15], df = 22, $t = -4.353$, $p < 0.001$) and central conditions (beta = −0.27, 95% CI = [−0.44, −0.09], df = 22, $t = -3.09$, $p < 0.01$) and similarly for beta in the peripheral (beta = −7.41, 95% CI = [−10,19., −5.15], df = 22, $t = -3.62$, $p < 0.01$) and central conditions (beta = −7.86, 95% CI = [−11,71., −4.02], df = 22, $t = -4.00$, $p < 0.001$). Lastly we compared the rate of misses (i.e., the amount of non-reactions or reactions that were larger than 1000 ms in relation to all target trials) between attention conditions, which showed no significant differences ($p > 0.28$). Nonetheless, the peripheral attention condition showed fewer misses ($M = 12.0\%$, SD = 12.2%) than the central attention one ($M = 15.9\%$, SD = 18.8%).

3.2 | Localizer

The localizer data showed a clearcut polarity reversal for stimulation of the UVF compared to the LVF (see Figure 2A,B). The maximal absolute value found within a 60–90 ms time window of the grand average of the POz electrode, used for C1 scoring in the standard analyses (uncorrected and corrected), had an amplitude of 3.71 μV and a latency of 89 ms. For the individualized analyses, we looked at the maximal amplitudes on occipital parietal electrodes per subject. The majority of participants showed a maximal C1 at the POz electrode ($n = 12$) and for a little less than half of the sample, a different electrode was found (see Figure 2D). As can be expected, mean peak amplitude (absolute value) across these electrodes was higher with ($M = 4.34$, SD = 1.61 μV) and the mean latency was earlier ($M = 85.1$, SD = 6.6 ms) than across only POz. Figure 2C also shows the distribution of optimal quadrants (i.e., the quadrant with peak amplitude in Pz, POz or Oz within 50–90 ms window) across participants that was used to adjust stimulus presentation in the main experiment.

3.3 | C1

3.3.1 | Uncorrected Data

We first modeled C1 amplitudes that were scored based on the standard approach (see Figure 3A1). The initial maximally fit model (AIC = 873.61, BIC = 934.28) was singular but explained the data significantly better than the simplified model (AIC = 927.38, BIC = 956.12; chi-squared = 73.77, df = 10, $p < 0.001$). It revealed a significant effect of visual field (beta = 2.898, 95% CI = [2.035, 3.762], df = 22.1, t-value = 6.58, $p < 0.001$). More importantly, this model showed a significant interaction between visual field and attention (beta = −0.300, 95%

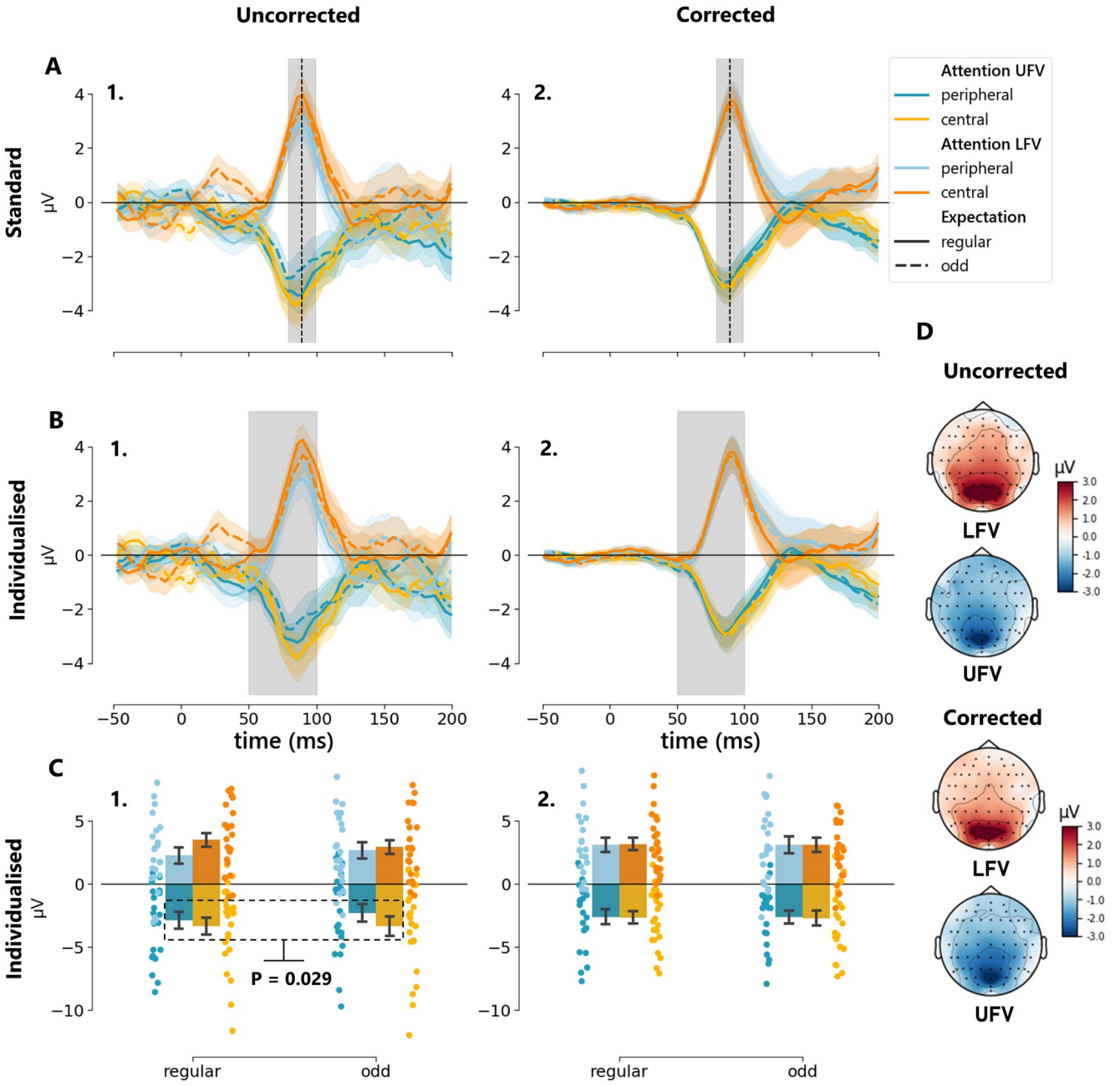

FIGURE 3 | Effects of attention and prediction on C1. (A, B) The grand average ERPs are shown, separately for each condition and visual field. (A) For the standard analysis, amplitudes were averaged over the POz electrode and C1 amplitude was scored as the mean amplitude within 79–99 ms (highlighted in gray), which was based on the grand average peak of the localizer. (B) For the individualized analysis, optimal electrodes and time windows (window range highlighted in gray) were selected separately for every participant. (A1, B1) Overlap-uncorrected ERP data. (A2, B2) Overlap-corrected ERP data. (C) The mean C1 amplitude for the individualized analysis for both corrected and uncorrected data is shown with bar plots and the participant means are shown with scatterplots. (D) The topographies of UVF and LVF stimuli at the peak latency are shown. Error bands and error bars indicate standard error of the mean.

CI = [−0.591, −0.008], df = 128.5, *t*-value = −2.017, $p = 0.046$). We therefore performed a follow-up analysis where two separate models were fit for the UFV and LVF. For the UVF model, the boundary was again singular and subsequent model comparison found no significant difference between model fits. Neither model showed a significant effect of attention ($p > 0.1$ in both cases). The same was true for the LVF, which showed no difference between the maximal and simplified model, and neither showed any significant effects of attention or prediction ($p > 0.1$).

For the individualized C1 amplitudes (see Figure 3B1), the maximal model (AIC = 853.7, BIC = 914.4) was singular but fit the data significantly better than a simplified model (AIC = 919.9, BIC = 948.6; Chi squared = 86.13, df = 10, $p < 0.001$). This model also revealed a significant effect of visual field (beta = 2.913, 95% CI = [2.048, 3.778], df = 22.1, *t*-value = 6.60, $p < 0.001$) and a significant interaction between attention and visual field (beta = −0.361, 95% CI = [−0.632, −0.090], df = 128.4, *t*-value = −2.61, $p = 0.010$). Notably, the follow-up maximal model

of the UVF was not singular and showed a significant effect of attention (beta = 0.378, 95% CI = [0.030, 0.725], df = 34.1, *t*-value = 2.13, $p = 0.040$). More specifically, this model showed a smaller C1 magnitude for peripheral attention ($M = -2.590$, SD = 3.154) than central attention ($M = -3.321$, SD = 3.466). For the LVF, we found a similar nonsignificant effect of attention (beta = −0.347, 95% CI = [−0.736, 0.042], df = 54.5; *t*-value = −1.74; $p = 0.086$), namely a smaller C1 magnitude for peripheral attention ($M = 2.478$, SD = 2.953) than central attention ($M = 3.227$, SD = 2.627).

3.3.2 | Overlap Corrected Data

When fitting the standard corrected data (see Figure 3A2), the maximal model (AIC = 734.0, BIC = 793.3) was singular but fit the data significantly better than a simplified model (AIC = 836.6, BIC = 864.7; Chi squared = 122.9, df = 10, $p < 0.001$) and found only an effect of visual field ($p < 0.001$) but no significant effects of attention, prediction, or interactions (all $p > 0.2$). As for the individualized corrected data (see Figure 3B2), again the initial model fit (AIC = 735.8, BIC = 795.2) was singular but fit the data better than the model (AIC = 844.9, BIC = 873.0; Chi squared = 129.1, df = 10, $p < 0.001$) but also showed no significant effects (all $p > 0.5$), except for visual field ($p < 0.001$).

3.4 | P1, N1, and P3

For the main analysis of P1 and N1 components, both maximal LMER models showed boundary issues and in both cases there were no clear differences in model fit between maximal and simple models. Visual inspection showed similar parameters for model assumptions. In both cases, we therefore selected the simplified models. The P1 model showed a significant main effect of attention (beta = 0.165, 95% CI = [0.0112, 0.3182], df = 62.3, $t = 2.10$, $p = 0.039$), revealing a larger P1 amplitude for peripheral ($M = 0.727\,\mu V$, SD = 1.610 μV) than central attention ($M = 0.292$, SD = 1.545) (see Figure 4). There were no other significant effects (all $p > 0.12$). For the N1, the model showed no significant effects (all $p > 0.25$).

For the analysis controlling for the hemisphere of P1 and N1 components, both models fit the data without boundary issues. The P1 model showed a main effect of attention (beta = 0.147, 95% CI = [0.0155, 0.2789], df = 22.5, $t = 2.19$, $p = 0.039$), revealing a larger P1 amplitude for peripheral ($M = 0.681\,\mu V$, SD = 1.685 μV) than central attention ($M = 0.368$, SD = 1.483) (see Figure 4). There were no other significant effects (all $p > 0.12$). For the N1, the model showed no significant effects (all $p > 0.45$), except for a significant main effect of hemisphere (beta = 0.182, df = 19.5, $t = 2.13$, $p = 0.046$).

For the P3 (see Figure 5), the maximal model was singular and the subsequent model comparison showed no significant difference between the maximal (AIC = 796.4, BIC = 831.3) and simplified model fit (AIC = 791.9, BIC = 817.3). Based on homogeneity of variance and linearity measures, the simplified model was found to better fit the data. This model contained the same fixed effects but only contained a random effects structure with a random slope for attention and a random intercept per subject. The analysis revealed a significant main effect of Prediction (beta = 0.2978, 95% CI = [0.0102, 0.5853], df = 130.0, $t = 2.030$, $p = 0.044$) with a smaller amplitude for regular trials ($M = 1.69\,\mu V$, SD = 1.86 μV) than odd trials ($M = 2.26\,\mu V$, SD = 2.88 μV; see Figure 5B). An exploratory follow-up analysis modeling attention conditions separately showed that this effect was mostly present in the peripheral attention condition (beta = 0.5233, 95% CI = [0.1248, 0.9217], df = 62.0, $t = 2.574$, $p = 0.0125$) but not in the central attention condition ($p > 0.7$).

4 | Discussion

The present ERP study aimed to investigate the influence of attention and prediction on the C1 component, thereby assessing if top-down mechanisms might influence feedforward sensory processing in V1 rapidly following stimulus onset. To this end, we devised a new paradigm where several methodological improvements were made compared to previous C1 studies. First and foremost, besides attention, we also manipulated prediction orthogonally (i.e., harnessing the principles of apparent motion, a specific location could be predicted by the participant regarding stimulus presentation), with the aim to assess whether complex interaction effects between these two processes could drive the C1 modulations, in keeping with previous fMRI studies that already documented such complex interaction effects (Alink et al. 2010; Kok, Jehee and de Lange 2012; Kok, Rahnev, et al. 2012; Richter and De Lange 2019). Moreover, using an independent localizer, we adjusted the stimulus presentation during the main experiment depending on the subject-specific expression of the C1 (likely reflecting V1 anatomy) to yield PEs at the location in the visual field where this retinotopic component was maximally expressed. We also used a gaze-contingent procedure, ensuring that the ERP data recorded were not contaminated by saccades toward the peripheral visual stimulus. Last but not least, using deconvolution, we also modeled and corrected overlapping ERP effects (from the preceding stimulus). A number of important new results emerge from this study.

With regard to the C1, our results highlight the dependence on particular analytical approaches (or choices) for the observation of attentional C1 effects. The analysis of the uncorrected data, for instance, highlights the difference between a standard and an individualized approach to the scoring and selection of C1 amplitude, as several previous studies have already established (Herde et al. 2022; Kelly et al. 2008; Proverbio et al. 2007; Wolf et al. 2022). More peculiarly, the application of linear deconvolution removed the modulation of the C1 by attention. This result is compatible with earlier ERP studies employing ADJAR as linear deconvolution (Woldorff 1993), who failed to reveal systematic effects of attention on the C1 (Clark and Hillyard 1996; Hillyard et al. 1998; Hopfinger and West 2006; Noesselt et al. 2002). Because ADJAR has strong limitations in its applicability, such as convergence issues leading to the loss of trials and a high computational cost (Kristensen et al. 2017; Talsma and Woldorff 2004), later studies that did find attentional C1 effects often opted for longer SOAs and did not perform any overlap correction (Herde et al. 2022; Kelly et al. 2008; Mohr et al. 2020; Wolf et al. 2022).

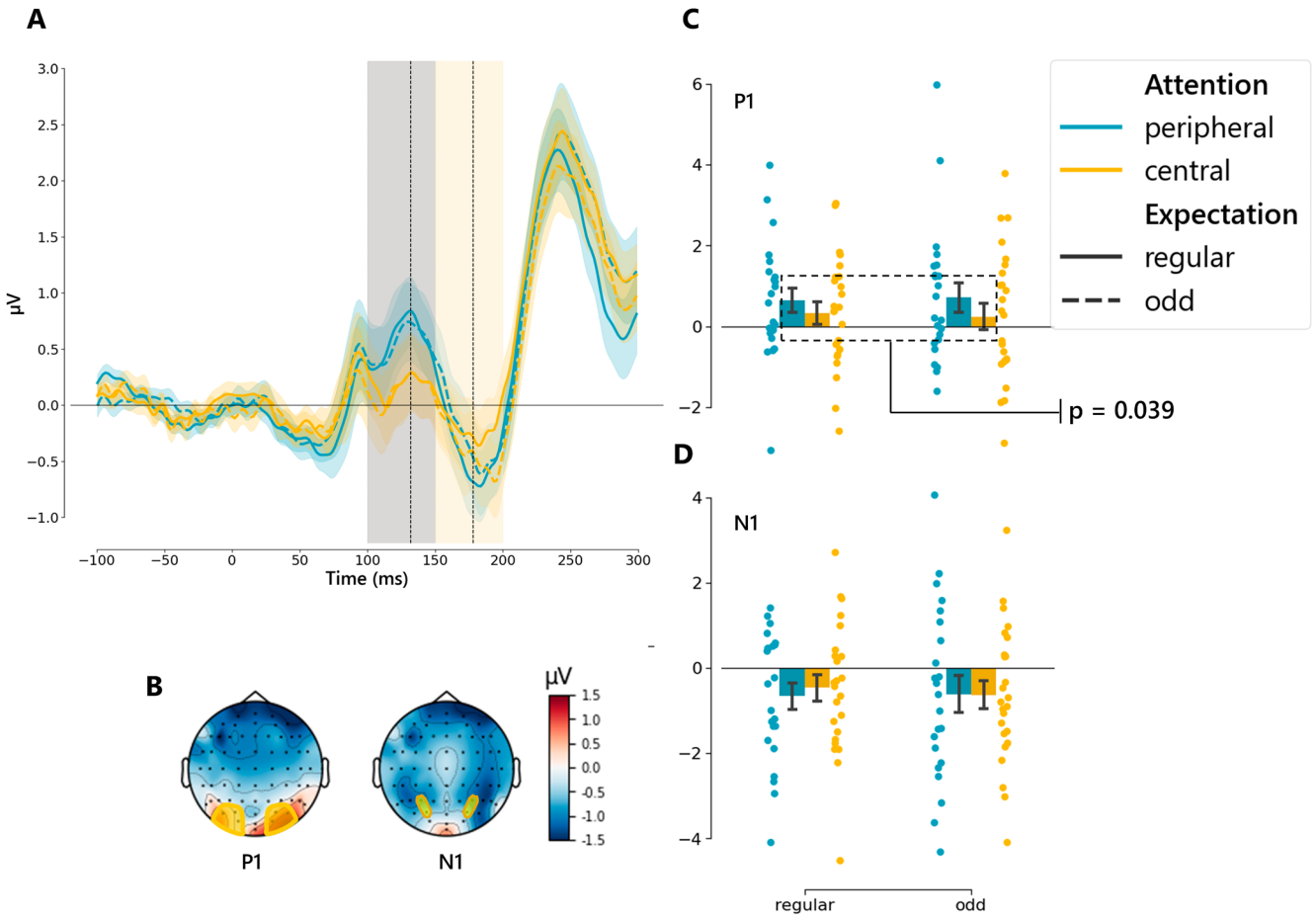

FIGURE 4 | Effects of attention and Prediction on P1 and N1 Components. (A) Grand average (and overlap-corrected) ERPs at lateral posterior electrodes (PO4, PO8, O2, PO3, PO7, and O1 combined), on which the P1 amplitude was scored. N1 amplitudes were scored on slightly more anterior electrodes (P04, P4, PO3 and P3). Nonetheless, peak selection ranges for both P1 and N1 components are shown, highlighted in gray and yellow, respectively. (B) The topography at the peak latency is shown for P1 (132 ms) and N1 (178 ms), with the selected electrodes highlighted in yellow. (C) A significant effect of attention was found for the P1 component. (D) No effect was found on the N1 component. Error bands and error bars indicate the standard error of the mean.

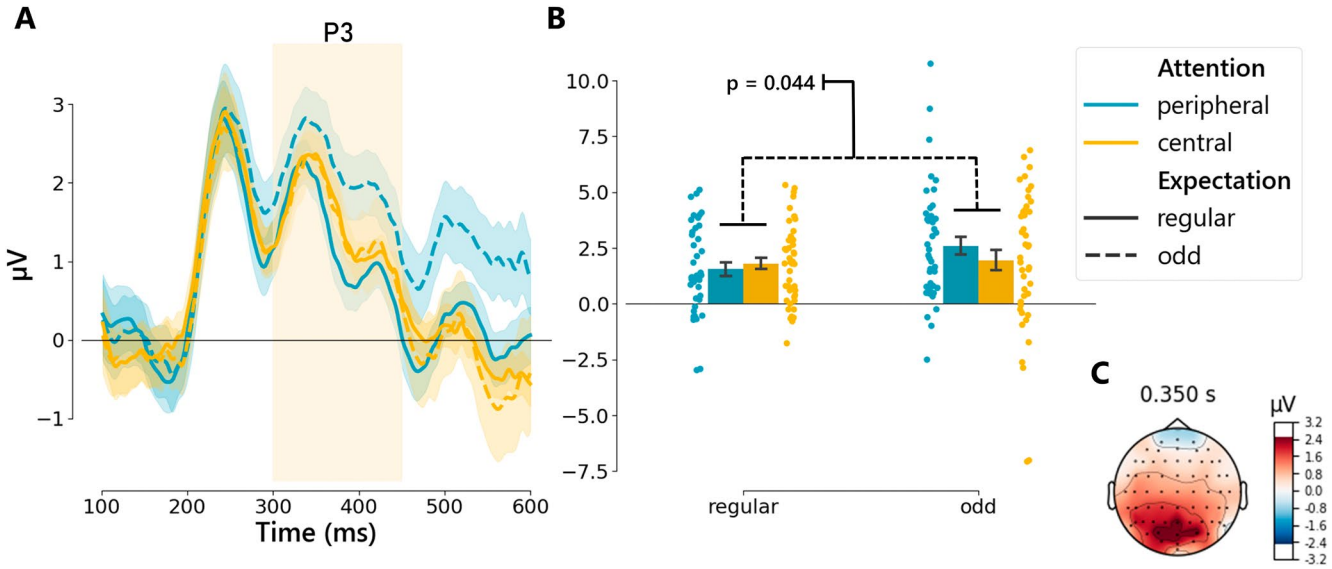

FIGURE 5 | Effects of attention and prediction on the P3 Component. (A) Grand average (and overlap-corrected) ERP waveforms for electrodes (Pz, POz, PO3 and PO4 combined) used to score P3. The P3 peak was selected within a 300–450 ms window following stimulus onset, highlighted in yellow. (B) A significant main effect of prediction was found for the P3. (C) The topography map shows the distribution at 350 ms after the stimulus. Error bands and error bars indicate the standard error of the mean.

One of the assumptions underlying linear deconvolution methods is that any given event induces an identical and temporarily fixed pattern of neural activity (Ehinger and Dimigen 2019; Smith and Kutas 2015). However, this means that temporally less defined pre-stimulus activity contributing to the original ERP is modeled away in the corrected signal, for instance by attributing it either to model residuals or to other modeled evoked activity from which the corrected signal is separated. The absence of attentional effects on the C1 in the overlap corrected data as opposed to the uncorrected ones in our experiment as well as in the existing literature, therefore, suggests that they might be driven by lingering or residual activities coming from the preceding stimulus (especially when a short SOA is used, as in our experiment) and/or by any other unaccounted pre-stimulus neural activity. The former is the most substantial reason for the use of these deconvolution methods in previous research (Clark and Hillyard 1996; Woldorff 1993). To formally assess this possibility, we also ran several control analyses informing (1) about what was the impact of the linear deconvolution correction (using Unfold) on our ERP data and (2) whether a residual activity from the preceding stimulus (and more specifically a P3 like activity) might indeed influence the C1 component (as well as later ERP components) for the current one or not (see Data S1 for details). However, in our case, because the attention manipulation was implemented at the block level instead of cueing at the single trial level, attention could be manifested as a sustained or preparatory process, which has been found to be reflected in activity such as the vN component (Di Russo et al. 2021) and pre-stimulus alpha (Bacigalupo and Luck 2019; Behzadnia et al. 2017; Doesburg et al. 2016; Worden et al. 2000) which in turn has also been found to contribute to early visually evoked components (Dou et al. 2022; Iemi et al. 2019; Samaha et al. 2015; Sauseng et al. 2007; Trajkovic et al. 2024). It is therefore possible that such activity could still be present in traditional ERPs but not in linearly deconvoluted rERPs.

It could be possible that a C1 effect is dependent on the interaction between ongoing post-perceptual pre-stimulus activity and the activity resulting from the presentation of a subsequent stimulus and that linear deconvolution could therefore remove or attenuate this effect. However, we argue that this is unlikely because the moment at which this potential collision occurs would be time-locked to the new stimulus as opposed to the preceding one. The resulting variance from this interaction would therefore be attributed by the model to the early time-course of the new stimulus as opposed to the end of the preceding one. We therefore believe that a true C1 effect, that results from an interaction between ongoing top-down attention and new stimulus information, would still be captured.

Although the stimuli were not optimized to elicit a strong P1 response, we found that this component, however, changed with our attention manipulation (i.e., it was larger for attended/peripheral than unattended/central stimuli), in agreement with many previous ERP studies available in the literature (e.g., Alilović et al. 2019; Clark and Hillyard 1996; Martínez et al. 2001; Marzecová et al. 2017; Wolf et al. 2022). However, because we did not report in parallel behavioral results confirming this assumption directly (given that we used an oddball design and collected few behavioral responses only to leave early visual ERPs unaffected by motor effects), this neurophysiological evidence (P1 effect) is and remains indirect, and this is a limitation of our study.

Moreover, the specifics of our attention manipulation, requiring the focus of attention to either be in the center of the screen or be distributed across the four locations in the periphery, did differ significantly from these previous studies. We employed this manipulation specifically to avoid the confounding of lateralization, and a control analysis did confirm that this P1 attention effect was not lateralized (i.e., the main effect of hemisphere or interaction between this factor and attention was not significant). However, the effect of this manipulation on P1 may therefore not only represent shifts in spatial attention but also the distance between the focus of attention and the stimulus, as this has been shown to influence P1 before (Mangun and Hillyard 1988).

Accordingly, it remains to be shown in future studies whether a more direct manipulation of spatial attention that engages more comparable regions of visual space, preferably corroborated by behavioral results as well, could influence the C1 component with the elected experimental design and these rotating stimuli. Because previous studies have reported a clear modulation of the C1 when more engaging tasks at the attentional level were used than in the present case (Fu et al. 2010; Kelly et al. 2008; Mohr et al. 2020; Slotnick 2018), we could reason that the absence of C1 modulation by attention in our study could partly be imputed to a weak manipulation of it, which involved only a partial or inconsistent engagement of top-down attentional control mechanisms. Accordingly, future ERP research is needed to assess whether the C1 could very well change in the current paradigm or not, when a more direct or straightforward manipulation of spatial attention is employed.

Furthermore, there were no effects on the N1 component (except for a main effect of hemisphere in the control analysis). This could be due to the very few target trials and relatively low task load. Indeed, previous studies have often employed more demanding target discrimination tasks to find attentional effects on the N1 component (Luck et al. 2000; Mangun et al. 2001; Marzecová et al. 2017). Lastly, both P1 and N1 components observed in this study were smaller than the typically observed response (e.g., Clark and Hillyard 1996; Luck et al. 2000; Martínez et al. 1999; Noesselt et al. 2002). This is likely due to the stimuli being optimized for C1 specific properties. Whereas the C1 gets larger when a stimulus has a high spatial frequency and is situated further in the periphery, the inverse is true for P1 and N1 (Clark et al. 1994; Ellemberg et al. 2001; Mangun and Hillyard 1988).

In our experiment, prediction did not influence these three early visual ERP components (C1, P1, and N1), but it did affect the P3 nonetheless, which is often considered to be indicative of post-perceptual and higher-order, amodal processing (Friedman et al. 2001; Polich 2007). Given its posterior parietal scalp distribution (see Figure 5), this P3 likely reflects "updating" upon change detection (Kamp 2020; Polich 2007). In agreement with this interpretation, previous ERP studies on predictive coding have reported correlations between the P3 amplitude and a computational "surprise" signal that is generated according to Bayesian inference of stimulus probability (Mars et al. 2008;

Meyniel et al. 2016). The P3 has been shown to be responsive to the frequency of a stimulus when participants are presented with a sequence of stimuli (Kamp 2020; Polich 2007; Polich and Bondurant 1997; Squires et al. 1976; Steiner et al. 2013). An infrequent stimulus, in this case, elicits a larger parietal positivity than a stimulus that has been encountered more often in the sequence, which is precisely the effect that we have observed here. The behavioral results of this experiment, as well as the control behavioral experiment (see Data S1), also corroborate this assumption, showing a higher sensitivity (d′) for regular than odd events. The exploratory follow-up analysis looking at peripheral and central attention conditions separately, however, indicates that this effect could be driven by a difference only in the peripheral and not in the central attention condition. This could be due to the prediction manipulation not being directly task-relevant in this central attention condition, as this condition required effectively no assessment of the peripheral stimuli. In comparison, P3 effects related to stimulus probability often require some kind of response to the infrequent stimulus (Gonsalvez and Polich 2002; Kamp 2020; Polich 2020; Steiner et al. 2013), though not always (Jeon and Polich 2001). This may also have been suboptimal for the detection of prediction effects on earlier evoked components, and indeed many previous studies have used relevant and more demanding tasks when looking at top-down influence on (Slotnick 2018). Nonetheless, this does not necessarily mean that predictable regularities are only processed when participants are actively attending them, as our behavioral results show that the difference in sensitivity (d′) between odd and regular trials remains present even when looking at attention conditions separately, which is in line with recent studies that have found participants to be sensitive to unexpected visual features without the direct allocation of attention (Center et al. 2024; Nartker et al. 2025).

Lastly, prediction was manipulated by changes in the rotational presentation pattern, which presumably induces apparent motion. Although previous fMRI research has shown that this type of prediction manipulation affects V1 activity (Alink et al. 2010; Edwards et al. 2017), motion itself is known to be mostly processed in higher levels of the visual cortical hierarchy, namely in area MT/V5+ (Bartels et al. 2008; Tootell et al. 1995; Zeki et al. 1991). Accordingly, the prediction of both real and apparent motion has been found to rely heavily on connections between V1 and MT/V5+ regions (Alink et al. 2010; Edwards et al. 2017; Vetter et al. 2015), though these seem to primarily consist of feedback projections from MT/V5+ to V1 (Muckli and Petro 2013; Sterzer et al. 2006; Vetter et al. 2015), which would not result in P1 or C1 effects. Even though the present rotational manipulation does indirectly infer a specific spatial position for the stimulus, which is a lower level property to which V1 is sensitive, and even though motion has been found to preactivate neural representations of anticipated spatial positions (Alilović et al. 2019; Blom et al. 2021; Hogendoorn and Burkitt 2018), the size of the receptive fields in the early visual system may be too small to initiate an early motion processing signal (Muckli et al. 2005; Smith et al. 2001), causing the evaluation of deviations of this motion to occur at a later stage. Instead of relying on motion, it could therefore be interesting for future research to employ prediction manipulations that address V1 specific properties directly, such as orientation or contrast, thereby activating local V1 pathways.

In conclusion, this study investigated top-down influences on early V1 activity by comparing spatial attention and prediction effects on the C1 component, as well as later visual ERPs. Our results reveal that attentional effects on the C1 component, but not the P1 component, are removed through the use of linear deconvolution, indicating that overlap from late ERP components and/or unaccounted pre-stimulus activity may be contributing factors to the observation of such effects. Furthermore, we found no evidence that apparent motion mechanisms can induce visible prediction effects on early visual ERPs, while it did influence the P3 component in our study. Prediction through motion processing may therefore primarily affect visual processing at a later stage following stimulus onset, possibly through delayed feedback projections from higher cortical areas. Overall, these findings highlight the importance of different analytical approaches to the observation of attentional effects on the C1, especially the use of linear deconvolution to counter short SOAs. Additionally, future studies should explore the use of prediction manipulations that directly target V1-specific properties to better understand the interplay of feedforward with feedback mechanisms in early vision.

Author Contributions

Maximilien Van Migem: conceptualization, investigation, data curation, software, methodology, writing – original draft, writing – review and editing, formal analysis, visualization. **Daniele Marinazzo:** conceptualization, writing – review and editing, funding acquisition, project administration, resources, supervision. **Gilles Pourtois:** conceptualization, methodology, supervision, resources, project administration, funding acquisition, writing – review and editing.

Acknowledgments

This project is funded by a grant from Ghent University—Special Research Fund (BOF.24Y.2023.0017.0) awarded to Gilles Pourtois and Daniele Marinazzo.

Funding

This project is funded by a grant from Ghent University—Special Research Fund (BOF.24Y.2023.0017.0) awarded to Gilles Pourtois and Daniele Marinazzo.

Conflicts of Interest

The authors declare no conflicts of interest.

Data Availability Statement

The raw data of this experiment are available upon request and all code used in this study for stimulus presentation, for pre-processing EEG data, for overlap correction, for figure plotting, and for statistical analyses can be found on GitHub via the following link: https://github.com/maxvanmigem/prediction-attention-v1-processing.

References

Aitken, F., G. Menelaou, O. Warrington, et al. 2020. "Prior Expectations Evoke Stimulus-Specific Activity in the Deep Layers of the Primary Visual Cortex." *PLoS Biology* 18, no. 12: e3001023. https://doi.org/10.1371/journal.pbio.3001023.

Ales, J. M., J. L. Yates, and A. Norcia. 2013. "On Determining the Intracranial Sources of Visual Evoked Potentials From Scalp

Topography: A Reply to Kelly et al. (This Issue)." *NeuroImage* 64: 703–711. https://doi.org/10.1016/j.neuroimage.2012.09.009.

Ales, J. M., J. L. Yates, and A. M. Norcia. 2010. "V1 Is Not Uniquely Identified by Polarity Reversals of Responses to Upper and Lower Visual Field Stimuli." *NeuroImage* 52, no. 4: 1401–1409. https://doi.org/10.1016/j.neuroimage.2010.05.016.

Alilović, J., B. Timmermans, L. C. Reteig, S. Van Gaal, and H. A. Slagter. 2019. "No Evidence That Predictions and Attention Modulate the First Feedforward Sweep of Cortical Information Processing." *Cerebral Cortex* 29, no. 5: 2261–2278. https://doi.org/10.1093/cercor/bhz038.

Alink, A., C. M. Schwiedrzik, A. Kohler, W. Singer, and L. Muckli. 2010. "Stimulus Predictability Reduces Responses in Primary Visual Cortex." *Journal of Neuroscience* 30, no. 8: 2960–2966. https://doi.org/10.1523/JNEUROSCI.3730-10.2010.

Bacigalupo, F., and S. J. Luck. 2019. "Lateralized Suppression of Alpha-Band EEG Activity as a Mechanism of Target Processing." *Journal of Neuroscience* 39, no. 5: 900–917. https://doi.org/10.1523/JNEUROSCI.0183-18.2018.

Barr, D. J., R. Levy, C. Scheepers, and H. J. Tily. 2013. "Random Effects Structure for Confirmatory Hypothesis Testing: Keep It Maximal." *Journal of Memory and Language* 68, no. 3: 255–278. https://doi.org/10.1016/j.jml.2012.11.001.

Bartels, A., S. Zeki, and N. K. Logothetis. 2008. "Natural Vision Reveals Regional Specialization to Local Motion and to Contrast-Invariant, Global Flow in the Human Brain." *Cerebral Cortex* 18, no. 3: 705–717. https://doi.org/10.1093/cercor/bhm107.

Bates, D., M. Mächler, B. Bolker, and S. Walker. 2015. "Fitting Linear Mixed-Effects Models Using lme4." *Journal of Statistical Software* 67, no. 1: 1–48. https://doi.org/10.18637/jss.v067.i01.

Baumgartner, H. M., C. J. Graulty, S. A. Hillyard, and M. A. Pitts. 2018. "Does Spatial Attention Modulate the Earliest Component of the Visual Evoked Potential?" *Cognitive Neuroscience* 9, no. 1–2: 4–19. https://doi.org/10.1080/17588928.2017.1333490.

Behzadnia, A., M. Ghoshuni, and S. A. Chermahini. 2017. "EEG Activities and the Sustained Attention Performance." *Neurophysiology* 49, no. 3: 226–233. https://doi.org/10.1007/s11062-017-9675-1.

Bezanson, J., A. Edelman, S. Karpinski, and V. B. Shah. 2017. "Julia: A Fresh Approach to Numerical Computing." *SIAM Review* 59, no. 1: 65–98. https://doi.org/10.1137/141000671.

Blom, T., S. Bode, and H. Hogendoorn. 2021. "The Time-Course of Prediction Formation and Revision in Human Visual Motion Processing." *Cortex* 138: 191–202. https://doi.org/10.1016/j.cortex.2021.02.008.

Center, E. G., K. D. Federmeier, and D. M. Beck. 2024. "The Brain's Sensitivity to Real-World Statistical Regularity Does Not Require Full Attention." *Journal of Cognitive Neuroscience* 36, no. 8: 1715–1740. https://doi.org/10.1162/jocn_a_02181.

Clark, A. 2013. "Whatever Next? Predictive Brains, Situated Agents, and the Future of Cognitive Science." *Behavioral and Brain Sciences* 36, no. 3: 181–204. https://doi.org/10.1017/S0140525X12000477.

Clark, V. P., S. Fan, and S. A. Hillyard. 1994. "Identification of Early Visual Evoked Potential Generators by Retinotopic and Topographic Analyses." *Human Brain Mapping* 2, no. 3: 170–187. https://doi.org/10.1002/hbm.460020306.

Clark, V. P., and S. A. Hillyard. 1996. "Spatial Selective Attention Affects Early Extrastriate but Not Striate Components of the Visual Evoked Potential." *Journal of Cognitive Neuroscience* 8, no. 5: 387–402. https://doi.org/10.1162/jocn.1996.8.5.387.

Dassanayake, T. L., P. T. Michie, and R. Fulham. 2016. "Effect of Temporal Predictability on Exogenous Attentional Modulation of Feedforward Processing in the Striate Cortex." *International Journal of Psychophysiology* 105: 9–16. https://doi.org/10.1016/j.ijpsycho.2016.04.007.

De Lange, F. P., M. Heilbron, and P. Kok. 2018. "How Do Expectations Shape Perception?" *Trends in Cognitive Sciences* 22, no. 9: 764–779. https://doi.org/10.1016/j.tics.2018.06.002.

Debes, S. R., and V. Dragoi. 2023. "Suppressing Feedback Signals to Visual Cortex Abolishes Attentional Modulation." *Science* 379, no. 6631: 468–473. https://doi.org/10.1126/science.ade1855.

Di Russo, F., M. Berchicci, V. Bianco, et al. 2021. "Sustained Visuospatial Attention Enhances Lateralized Anticipatory ERP Activity in Sensory Areas." *Brain Structure and Function* 226, no. 2: 457–470. https://doi.org/10.1007/s00429-020-02192-6.

Di Russo, F., A. Martínez, M. I. Sereno, S. Pitzalis, and S. A. Hillyard. 2002. "Cortical Sources of the Early Components of the Visual Evoked Potential." *Human Brain Mapping* 15, no. 2: 95–111. https://doi.org/10.1002/hbm.10010.

Doesburg, S. M., N. Bedo, and L. M. Ward. 2016. "Top-Down Alpha Oscillatory Network Interactions During Visuospatial Attention Orienting." *NeuroImage* 132: 512–519. https://doi.org/10.1016/j.neuroimage.2016.02.076.

Doricchi, F., S. Lasaponara, M. Pazzaglia, and M. Silvetti. 2022. "Left and Right Temporal-Parietal Junctions (TPJs) as "Match/Mismatch" Hedonic Machines: A Unifying Account of TPJ Function." *Physics of Life Reviews* 42: 56–92. https://doi.org/10.1016/j.plrev.2022.07.001.

Dou, W., A. Morrow, L. Iemi, and J. Samaha. 2022. "Pre-Stimulus Alpha-Band Phase Gates Early Visual Cortex Responses." *NeuroImage* 253: 119060. https://doi.org/10.1016/j.neuroimage.2022.119060.

Edwards, G., P. Vetter, F. McGruer, L. S. Petro, and L. Muckli. 2017. "Predictive Feedback to V1 Dynamically Updates With Sensory Input." *Scientific Reports* 7, no. 1: 16538. https://doi.org/10.1038/s41598-017-16093-y.

Egner, T., J. M. Monti, and C. Summerfield. 2010. "Expectation and Surprise Determine Neural Population Responses in the Ventral Visual Stream." *Journal of Neuroscience* 30, no. 49: 16601–16608. https://doi.org/10.1523/JNEUROSCI.2770-10.2010.

Ehinger, B., and P. Alday. 2025. "Unfold.Jl: Event-Related Regression Toolbox (Version v0.8.1) [Computer Software]." Zenodo. https://doi.org/10.5281/ZENODO.14652576.

Ehinger, B., and O. Dimigen. 2019. "Unfold: An Integrated Toolbox for Overlap Correction, Non-Linear Modeling, and Regression-Based EEG Analysis." *PeerJ* 7: e7838. https://doi.org/10.7717/peerj.7838.

Ekroll, V., F. Faul, and J. Golz. 2008. "Classification of Apparent Motion Percepts Based on Temporal Factors." *Journal of Vision* 8, no. 4: 31. https://doi.org/10.1167/8.4.31.

Ellemberg, D., B. Hammarrenger, F. Lepore, M.-S. Roy, and J.-P. Guillemot. 2001. "Contrast Dependency of VEPs as a Function of Spatial Frequency: The Parvocellular and Magnocellular Contributions to Human VEPs." *Spatial Vision* 15, no. 1: 99–111. https://doi.org/10.1163/15685680152692042.

Faul, F., E. Erdfelder, A.-G. Lang, and A. Buchner. 2007. "G*Power 3: A Flexible Statistical Power Analysis Program for the Social, Behavioral, and Biomedical Sciences." *Behavior Research Methods* 39, no. 2: 175–191. https://doi.org/10.3758/BF03193146.

Foxe, J., and G. Simpson. 2002. "Flow of Activation From V1 to Frontal Cortex in Humans." *Experimental Brain Research* 142, no. 1: 139–150. https://doi.org/10.1007/s00221-001-0906-7.

Foxe, J., E. C. Strugstad, P. Sehatpour, et al. 2008. "Parvocellular and Magnocellular Contributions to the Initial Generators of the Visual Evoked Potential: High-Density Electrical Mapping of the "C1" Component." *Brain Topography* 21, no. 1: 11–21. https://doi.org/10.1007/s10548-008-0063-4.

Friedman, D., Y. M. Cycowicz, and H. Gaeta. 2001. "The Novelty P3: An Event-Related Brain Potential (ERP) Sign of the Brain's Evaluation of Novelty." *Neuroscience & Biobehavioral Reviews* 25, no. 4: 355–373. https://doi.org/10.1016/S0149-7634(01)00019-7.

Friston, K. 2009. "The Free-Energy Principle: A Rough Guide to the Brain?" *Trends in Cognitive Sciences* 13, no. 7: 293–301. https://doi.org/10.1016/j.tics.2009.04.005.

Fu, S., J. Fedota, P. M. Greenwood, and R. Parasuraman. 2010. "Early Interaction Between Perceptual Load and Involuntary Attention: An Event-Related Potential Study." *Neuroscience Letters* 468, no. 1: 68–71. https://doi.org/10.1016/j.neulet.2009.10.065.

Fu, S., Y. Huang, Y. Luo, et al. 2009. "Perceptual Load Interacts With Involuntary Attention at Early Processing Stages: Event-Related Potential Studies." *NeuroImage* 48, no. 1: 191–199. https://doi.org/10.1016/j.neuroimage.2009.06.028.

Gebodh, N., M. I. Vanegas, and S. P. Kelly. 2017. "Effects of Stimulus Size and Contrast on the Initial Primary Visual Cortical Response in Humans." *Brain Topography* 30, no. 4: 450–460. https://doi.org/10.1007/s10548-016-0530-2.

Gilbert, C. D., and W. Li. 2013. "Top-Down Influences on Visual Processing." *Nature Reviews Neuroscience* 14, no. 5: 350–363. https://doi.org/10.1038/nrn3476.

Gonsalvez, C. J., and J. Polich. 2002. "P300 Amplitude Is Determined by Target-to-Target Interval." *Psychophysiology* 39, no. 3: 388–396. https://doi.org/10.1017/S0048577201393137.

Gramfort, A. 2013. "MEG and EEG Data Analysis With MNE-Python." *Frontiers in Neuroscience* 7: 267. https://doi.org/10.3389/fnins.2013.00267.

Hautus, M. J. 1995. "Corrections for Extreme Proportions and Their Biasing Effects on Estimated Values Ofd." *Behavior Research Methods, Instruments, & Computers* 27, no. 1: 46–51. https://doi.org/10.3758/BF03203619.

Hautus, M. J., N. A. Macmillan, and C. D. Creelman. 2021. *Detection Theory: A User's Guide*. 3rd ed. Routledge. https://doi.org/10.4324/9781003203636.

Herde, L., V. Rossi, G. Pourtois, and K. Rauss. 2018. "Early Retinotopic Responses to Violations of Emotion–Location Associations May Depend on Conscious Awareness." *Cognitive Neuroscience* 9, no. 1–2: 38–55. https://doi.org/10.1080/17588928.2017.1338250.

Herde, L., M. Schönauer-Firle, and K. Rauss. 2022. "Retinotopically Specific Effects of Attention on Human Early Visual Cortex Activity." *Journal of Experimental Psychology: Human Perception and Performance* 48, no. 8: 856–870. https://doi.org/10.1037/xhp0001022.

Hillyard, S. A., E. K. Vogel, and S. J. Luck. 1998. "Sensory Gain Control (Amplification) as a Mechanism of Selective Attention: Electrophysiological and Neuroimaging Evidence." *Philosophical Transactions of the Royal Society of London. Series B: Biological Sciences* 353, no. 1373: 1257–1270. https://doi.org/10.1098/rstb.1998.0281.

Hogendoorn, H., and A. N. Burkitt. 2018. "Predictive Coding of Visual Object Position Ahead of Moving Objects Revealed by Time-Resolved EEG Decoding." *NeuroImage* 171: 55–61. https://doi.org/10.1016/j.neuroimage.2017.12.063.

Hopfinger, J. B., and V. M. West. 2006. "Interactions Between Endogenous and Exogenous Attention on Cortical Visual Processing." *NeuroImage* 31, no. 2: 774–789. https://doi.org/10.1016/j.neuroimage.2005.12.049.

Iemi, L., N. A. Busch, A. Laudini, et al. 2019. "Multiple Mechanisms Link Prestimulus Neural Oscillations to Sensory Responses." *eLife* 8: e43620. https://doi.org/10.7554/eLife.43620.

Jeffreys, D. A., and J. G. Axford. 1972. "Source Locations of Pattern-Specific Components of Human Visual Evoked Potentials. I. Component of Striate Cortical Origin." *Experimental Brain Research* 16, no. 1: 1–21. https://doi.org/10.1007/BF00233371.

Jeon, Y.-W., and J. Polich. 2001. "P3a From a Passive Visual Stimulus Task." *Clinical Neurophysiology* 112, no. 12: 2202–2208. https://doi.org/10.1016/S1388-2457(01)00663-0.

Kamp, S. 2020. "Preceding Stimulus Sequence Effects on the Oddball-P300 in Young and Healthy Older Adults." *Psychophysiology* 57, no. 7: e13593. https://doi.org/10.1111/psyp.13593.

Kapadia, M. K., M. Ito, C. D. Gilbert, and G. Westheimer. 1995. "Improvement in Visual Sensitivity by Changes in Local Context: Parallel Studies in Human Observers and in V1 of Alert Monkeys." *Neuron* 15, no. 4: 843–856. https://doi.org/10.1016/0896-6273(95)90175-2.

Kelly, S. P., M. Gomez-Ramirez, and J. J. Foxe. 2008. "Spatial Attention Modulates Initial Afferent Activity in Human Primary Visual Cortex." *Cerebral Cortex* 18, no. 11: 2629–2636. https://doi.org/10.1093/cercor/bhn022.

Kelly, S. P., C. E. Schroeder, and E. C. Lalor. 2013. "What Does Polarity Inversion of Extrastriate Activity Tell Us About Striate Contributions to the Early VEP? A Comment on Ales Et al. (2010)." *NeuroImage* 76: 442–445. https://doi.org/10.1016/j.neuroimage.2012.03.081.

Kelly, S. P., M. I. Vanegas, C. E. Schroeder, and E. C. Lalor. 2013. "The Cruciform Model of Striate Generation of the Early VEP, Re-Illustrated, Not Revoked: A Reply to Ales Et al. (2013)." *NeuroImage* 82: 154–159. https://doi.org/10.1016/j.neuroimage.2013.05.112.

Kenemans, J. L., J. M. P. Baas, G. R. Mangun, M. Lijffijt, and M. N. Verbaten. 2000. "On the Processing of Spatial Frequencies as Revealed by Evoked-Potential Source Modeling." *Clinical Neurophysiology* 111, no. 6: 1113–1123. https://doi.org/10.1016/S1388-2457(00)00270-4.

Knight, R. T., D. Scabini, D. L. Woods, and C. C. Clayworth. 1989. "Contributions of Temporal-Parietal Junction to the Human Auditory P3." *Brain Research* 502, no. 1: 109–116. https://doi.org/10.1016/0006-8993(89)90466-6.

Kok, P., M. F. Failing, and F. P. De Lange. 2014. "Prior Expectations Evoke Stimulus Templates in the Primary Visual Cortex." *Journal of Cognitive Neuroscience* 26, no. 7: 1546–1554. https://doi.org/10.1162/jocn_a_00562.

Kok, P., J. F. M. Jehee, and F. P. de Lange. 2012. "Less Is More: Expectation Sharpens Representations in the Primary Visual Cortex." *Neuron* 75, no. 2: 265–270. https://doi.org/10.1016/j.neuron.2012.04.034.

Kok, P., D. Rahnev, J. F. M. Jehee, H. C. Lau, and F. P. De Lange. 2012. "Attention Reverses the Effect of Prediction in Silencing Sensory Signals." *Cerebral Cortex* 22, no. 9: 2197–2206. https://doi.org/10.1093/cercor/bhr310.

Kolers, P. A. 1963. "Some Differences Between Real and Apparent Visual Movement." *Vision Research* 3, no. 5–6: 191–206.

Kristensen, E., B. Rivet, and A. Guérin-Dugué. 2017. "Estimation of Overlapped Eye Fixation Related Potentials: The General Linear Model, a More Flexible Framework Than the ADJAR Algorithm." *Journal of Eye Movement Research* 10, no. 1: 1–27. https://doi.org/10.16910/jemr.10.1.7.

Kuznetsova, A., P. B. Brockhoff, and R. H. B. Christensen. 2017. "lmerTest Package: Tests in Linear Mixed Effects Models." *Journal of Statistical Software* 82, no. 13: 1–26. https://doi.org/10.18637/jss.v082.i13.

Lamme, V. A. F., and P. R. Roelfsema. 2000. "The Distinct Modes of Vision Offered by Feedforward and Recurrent Processing." *Trends in Neurosciences* 23, no. 11: 571–579. https://doi.org/10.1016/S0166-2236(00)01657-X.

Larson, E., A. Gramfort, D. A. Engemann, et al. 2023. ""MNE-Python (Version v1.3.1)." [Computer software]. *Zenodo*. https://doi.org/10.5281/ZENODO.7671973.

Luck, S. J., G. F. Woodman, and E. K. Vogel. 2000. "Event-Related Potential Studies of Attention." *Trends in Cognitive Sciences* 4, no. 11: 432–440. https://doi.org/10.1016/S1364-6613(00)01545-X.

Lüdecke, D., M. Ben-Shachar, I. Patil, P. Waggoner, and D. Makowski. 2021. "Performance: An R Package for Assessment, Comparison and Testing of Statistical Models." *Journal of Open Source Software* 6, no. 60: 3139. https://doi.org/10.21105/joss.03139.

Mangun, G. R., and S. A. Hillyard. 1988. "Spatial Gradients of Visual Attention: Behavioral and Electrophysiological Evidence." *Electroencephalography and Clinical Neurophysiology* 70, no. 5: 417–428. https://doi.org/10.1016/0013-4694(88)90019-3.

Mangun, G. R., H. Hinrichs, M. Scholz, et al. 2001. "Integrating Electrophysiology and Neuroimaging of Spatial Selective Attention to Simple Isolated Visual Stimuli." *Vision Research* 41, no. 10–11: 1423–1435. https://doi.org/10.1016/S0042-6989(01)00046-3.

Mars, R. B., S. Debener, T. E. Gladwin, et al. 2008. "Trial-By-Trial Fluctuations in the Event-Related Electroencephalogram Reflect Dynamic Changes in the Degree of Surprise." *Journal of Neuroscience* 28, no. 47: 12539–12545. https://doi.org/10.1523/JNEUROSCI.2925-08.2008.

Martínez, A., L. Anllo-Vento, M. I. Sereno, et al. 1999. "Involvement of Striate and Extrastriate Visual Cortical Areas in Spatial Attention." *Nature Neuroscience* 2, no. 4: 364–369. https://doi.org/10.1038/7274.

Martínez, A., F. DiRusso, L. Anllo-Vento, M. I. Sereno, R. B. Buxton, and S. A. Hillyard. 2001. "Putting Spatial Attention on the Map: Timing and Localization of Stimulus Selection Processes in Striate and Extrastriate Visual Areas." *Vision Research* 41, no. 10–11: 1437–1457. https://doi.org/10.1016/S0042-6989(00)00267-4.

Marzecová, A., A. Widmann, I. SanMiguel, S. A. Kotz, and E. Schröger. 2017. "Interrelation of Attention and Prediction in Visual Processing: Effects of Task-Relevance and Stimulus Probability." *Biological Psychology* 125: 76–90. https://doi.org/10.1016/j.biopsycho.2017.02.009.

Matuschek, H., R. Kliegl, S. Vasishth, H. Baayen, and D. Bates. 2017. "Balancing Type I Error and Power in Linear Mixed Models." *Journal of Memory and Language* 94: 305–315. https://doi.org/10.1016/j.jml.2017.01.001.

Meyniel, F., M. Maheu, and S. Dehaene. 2016. "Human Inferences About Sequences: A Minimal Transition Probability Model." *PLoS Computational Biology* 12, no. 12: e1005260. https://doi.org/10.1371/journal.pcbi.1005260.

Mohr, K. S., N. Carr, R. Georgel, and S. P. Kelly. 2020. "Modulation of the Earliest Component of the Human VEP by Spatial Attention: An Investigation of Task Demands." *Cerebral Cortex Communications* 1, no. 1: tgaa045. https://doi.org/10.1093/texcom/tgaa045.

Mohr, K. S., A. C. Geuzebroek, and S. P. Kelly. 2024. "Visual Cortical Area Contributions to the Transient, Multifocal and Steady-State VEP: A Forward Model-Informed Analysis." *Imaging Neuroscience* 2: 00152. https://doi.org/10.1162/imag_a_00152.

Muckli, L., A. Kohler, N. Kriegeskorte, and W. Singer. 2005. "Primary Visual Cortex Activity Along the Apparent-Motion Trace Reflects Illusory Perception." *PLoS Biology* 3, no. 8: e265. https://doi.org/10.1371/journal.pbio.0030265.

Muckli, L., and L. S. Petro. 2013. "Network Interactions: Non-Geniculate Input to V1." *Current Opinion in Neurobiology* 23, no. 2: 195–201. https://doi.org/10.1016/j.conb.2013.01.020.

Nartker, M., C. Firestone, H. Egeth, and I. Phillips. 2025. "Sensitivity to Visual Features in Inattentional Blindness." *eLife* 13: RP100337. https://doi.org/10.7554/eLife.100337.

Noesselt, T., S. A. Hillyard, M. G. Woldorff, et al. 2002. "Delayed Striate Cortical Activation During Spatial Attention." *Neuron* 35, no. 3: 575–587. https://doi.org/10.1016/S0896-6273(02)00781-X.

Peirce, J., J. R. Gray, S. Simpson, et al. 2019. "PsychoPy2: Experiments in Behavior Made Easy." *Behavior Research Methods* 51, no. 1: 195–203. https://doi.org/10.3758/s13428-018-01193-y.

Pitts, M. A., A. Martinez, and S. A. Hillyard. 2010. "When and Where Is Binocular Rivalry Resolved in the Visual Cortex?" *Journal of Vision* 10, no. 14: 25. https://doi.org/10.1167/10.14.25.

Polich, J. 2007. "Updating P300: An Integrative Theory of P3a and P3b." *Clinical Neurophysiology* 118, no. 10: 2128–2148. https://doi.org/10.1016/j.clinph.2007.04.019.

Polich, J. 2020. "50+Years of P300: Where are We Now?" *Psychophysiology* 57, no. 7: e13616. https://doi.org/10.1111/psyp.13616.

Polich, J., and T. Bondurant. 1997. "P300 Sequence Effects, Probability, and Interstimulus Interval." *Physiology & Behavior* 61, no. 6: 843–849. https://doi.org/10.1016/S0031-9384(96)00564-1.

Proverbio, A. M., M. Del Zotto, and A. Zani. 2007. "Inter-Individual Differences in the Polarity of Early Visual Responses and Attention Effects." *Neuroscience Letters* 419, no. 2: 131–136. https://doi.org/10.1016/j.neulet.2007.04.048.

Proverbio, A. M., M. Del Zotto, and A. Zani. 2010. "Electrical Neuroimaging Evidence That Spatial Frequency-Based Selective Attention Affects V1 Activity as Early as 40–60 Ms in Humans." *BMC Neuroscience* 11, no. 1: 59. https://doi.org/10.1186/1471-2202-11-59.

Qin, N., F. Crespi, A. M. Proverbio, and G. Pourtois. 2023. "A Systematic Exploration of Attentional Load Effects on the C1 ERP Component." *Psychophysiology* 60, no. 6: e14301. https://doi.org/10.1111/psyp.14301.

Qin, N., S. Wiens, K. Rauss, and G. Pourtois. 2022. "Effects of Selective Attention on the C1 ERP Component: A Systematic Review and Meta-Analysis." *Psychophysiology* 59, no. 12: e14123. https://doi.org/10.1111/psyp.14123.

R Core Team. 2022. *R: A Language and Environment for Statistical Computing (Version 4.2.0)*. R Foundation for Statistical Computing. https://www.R-project.org/.

Rao, R. P. N., and D. H. Ballard. 1999. "Predictive Coding in the Visual Cortex: A Functional Interpretation of Some Extra-Classical Receptive-Field Effects." *Nature Neuroscience* 2, no. 1: 79–87. https://doi.org/10.1038/4580.

Rauss, K., S. Schwartz, and G. Pourtois. 2011. "Top-Down Effects on Early Visual Processing in Humans: A Predictive Coding Framework." *Neuroscience & Biobehavioral Reviews* 35, no. 5: 1237–1253. https://doi.org/10.1016/j.neubiorev.2010.12.011.

Richter, D., and F. P. De Lange. 2019. "Statistical Learning Attenuates Visual Activity Only for Attended Stimuli." *eLife* 8: e47869. https://doi.org/10.7554/eLife.47869.

Rossi, V., and G. Pourtois. 2012. "State-Dependent Attention Modulation of Human Primary Visual Cortex: A High Density ERP Study." *NeuroImage* 60, no. 4: 2365–2378. https://doi.org/10.1016/j.neuroimage.2012.02.007.

Rossi, V., and G. Pourtois. 2014. "Electrical Neuroimaging Reveals Content-Specific Effects of Threat in Primary Visual Cortex and Fronto-Parietal Attentional Networks." *NeuroImage* 98: 11–22. https://doi.org/10.1016/j.neuroimage.2014.04.064.

Samaha, J., P. Bauer, S. Cimaroli, and B. R. Postle. 2015. "Top-Down Control of the Phase of Alpha-Band Oscillations as a Mechanism for Temporal Prediction." *Proceedings of the National Academy of Sciences* 112, no. 27: 8439–8444. https://doi.org/10.1073/pnas.1503686112.

Sauseng, P., W. Klimesch, W. R. Gruber, S. Hanslmayr, R. Freunberger, and M. Doppelmayr. 2007. "Are Event-Related Potential Components Generated by Phase Resetting of Brain Oscillations? A Critical Discussion." *Neuroscience* 146, no. 4: 1435–1444. https://doi.org/10.1016/j.neuroscience.2007.03.014.

Simpson, A. J., and M. J. Fitter. 1973. "What Is the Best Index of Detectability?" *Psychological Bulletin* 80, no. 6: 481–488. https://doi.org/10.1037/h0035203.

Skukies, R., and B. V. Ehinger. 2023. "The Effect of Estimation Time Window Length on Overlap Correction in EEG Data." https://doi.org/10.1101/2023.06.05.543689.

Slotnick, S. D. 2018. "The Experimental Parameters That Affect Attentional Modulation of the ERP C1 Component." *Cognitive Neuroscience* 9, no. 1–2: 53–62. https://doi.org/10.1080/17588928.2017.1369021.

Smith, A. T., K. D. Singh, K. L. Williams, and M. W. Greenlee. 2001. "Estimating Receptive Field Size From fMRI Data in Human Striate and Extrastriate Visual Cortex." *Cerebral Cortex* 11, no. 12: 1182–1190. https://doi.org/10.1093/cercor/11.12.1182.

Smith, N. J., and M. Kutas. 2015. "Regression-Based Estimation of ERP Waveforms: I the rERP Framework." *Psychophysiology* 52, no. 2: 157–168. https://doi.org/10.1111/psyp.12317.

Squires, K. C., C. Wickens, N. K. Squires, and E. Donchin. 1976. "The Effect of Stimulus Sequence on the Waveform of the Cortical Event-Related Potential." *Science* 193, no. 4258: 1142–1146. https://doi.org/10.1126/science.959831.

Steiner, G. Z., R. J. Barry, and C. J. Gonsalvez. 2013. "Can Working Memory Predict Target-to-Target Interval Effects in the P300?" *International Journal of Psychophysiology* 89, no. 3: 399–408. https://doi.org/10.1016/j.ijpsycho.2013.07.011.

Sterzer, P., J.-D. Haynes, and G. Rees. 2006. "Primary Visual Cortex Activation on the Path of Apparent Motion Is Mediated by Feedback From hMT+/V5." *NeuroImage* 32, no. 3: 1308–1316. https://doi.org/10.1016/j.neuroimage.2006.05.029.

Summerfield, C., and T. Egner. 2009. "Expectation (And Attention) in Visual Cognition." *Trends in Cognitive Sciences* 13, no. 9: 403–409. https://doi.org/10.1016/j.tics.2009.06.003.

Talsma, D., and M. G. Woldorff. 2004. "Methods for the Estimation and Removal of Artifacts and Overlap in ERP Data." In *Event-Related Potentials: A Methods Handbook*, edited by T. Handy. MIT Press.

Thomas, E. R., J. Haarsma, J. Nicholson, D. Yon, P. Kok, and C. Press. 2024. "Predictions and Errors are Distinctly Represented Across V1 Layers." *Current Biology* 34, no. 10: 2265–2271.e4. https://doi.org/10.1016/j.cub.2024.04.036.

Tootell, R., J. Reppas, K. Kwong, et al. 1995. "Functional Analysis of Human MT and Related Visual Cortical Areas Using Magnetic Resonance Imaging." *Journal of Neuroscience* 15, no. 4: 3215–3230. https://doi.org/10.1523/JNEUROSCI.15-04-03215.1995.

Trajkovic, J., F. Di Gregorio, G. Thut, and V. Romei. 2024. "Transcranial Magnetic Stimulation Effects Support an Oscillatory Model of ERP Genesis." *Current Biology* 34: 1048–1058.e4. https://doi.org/10.1016/j.cub.2024.01.069.

Vetter, P., M.-H. Grosbras, and L. Muckli. 2015. "TMS Over V5 Disrupts Motion Prediction." *Cerebral Cortex* 25, no. 4: 1052–1059. https://doi.org/10.1093/cercor/bht297.

Woldorff, M. G. 1993. "Distortion of ERP Averages due to Overlap From Temporally Adjacent ERPs: Analysis and Correction." *Psychophysiology* 30, no. 1: 98–119. https://doi.org/10.1111/j.1469-8986.1993.tb03209.x.

Wolf, M.-I., M. Bruchmann, G. Pourtois, S. Schindler, and T. Straube. 2022. "Top-Down Modulation of Early Visual Processing in V1: Dissociable Neurophysiological Effects of Spatial Attention, Attentional Load and Task-Relevance." *Cerebral Cortex* 32, no. 10: 2112–2128. https://doi.org/10.1093/cercor/bhab342.

Worden, M. S., J. J. Foxe, N. Wang, and G. V. Simpson. 2000. "Anticipatory Biasing of Visuospatial Attention Indexed by Retinotopically Specific α-Bank Electroencephalography Increases Over Occipital Cortex." *Journal of Neuroscience* 20, no. 6: RC63. https://doi.org/10.1523/JNEUROSCI.20-06-j0002.2000.

Zeki, S., J. Watson, C. Lueck, K. Friston, C. Kennard, and R. Frackowiak. 1991. "A Direct Demonstration of Functional Specialization in Human Visual Cortex." *Journal of Neuroscience* 11, no. 3: 641–649. https://doi.org/10.1523/JNEUROSCI.11-03-00641.1991.

Supporting Information

Additional supporting information can be found online in the Supporting Information section. **Data S1:** psyp70219-sup-0001-DataS1.docx.